PH-RESPONSIVE POLYMERIC MATERIALS FOR ENCAPSULATION AND TRIGGERED RELEASE

BY

HSUAN-CHIN WANG

DISSERTATION

Submitted in partial fulfillment of the requirements
for the degree of Doctor of Philosophy in Chemistry
in the Graduate College of the
University of Illinois at Urbana-Champaign, 2017

Urbana, Illinois

Doctoral Committee:

Professor Steven C. Zimmerman, Chair
Professor Paul V. Braun
Professor Jianjun Cheng
Professor Nancy R. Sottos

Abstract

The strong research interest in encapsulation chemistry for functional chemical species (commonly referred to as active ingredients or actives) arises from the need to devise tailored strategies to protect precious actives from premature degradation or leakage. Furthermore, to maximize the performance of the encapsulated actives, a controllable method is needed to release the materials at the desired time, location, and rate. To address these challenges, scientists look to stimuli-responsive polymers as a solution because polymers can be designed with tailored properties thanks to advancement in polymer chemistry and engineering. This dissertation discloses a collaborative effort between the Zimmerman group and Dow Chemical to develop novel pH-responsive polymeric materials for encapsulation and triggered-release.

As a release trigger, pH is attractive because of the prevalence of environments with specific pH levels. In the first part of the dissertation, a diester diacid chloride monomer, PDDC, was utilized in the preparation of a novel pH-responsive polyamide microcapsule. PDDC was selected for its susceptibility to hydrolysis as well as simplicity in structure and synthesis. A mixture of polyamine monomers, which includes a triazine trisamine crosslinker and the commercially available DETA, reacted with PDDC to afford toluene-loaded (ca. 95% by weight), free-flowing microcapsules through interfacial polymerization. Through dye release experiments, the triazine-DETA-PDDC microcapsules exhibited a unique pH-dependent release behavior: similarly fast, first order like release profiles at pH 5 and pH 10 and a steady, linear release profile at pH 7.4. In a dry or hydrophobic environment, the microcapsules remained stable without UV-Vis detectable dye release or rapid loss of the volatile core solvent. In summary, the

PDDC polyamide chemistry utilizes a single set of synthetically scalable monomers to prepare multi-pH responsive microcapsules that could see applications in different pH environments.

The second portion of the dissertation concerns a novel polyacetal that utilizes an intramolecular mechanism to facilitate depolymerization in a low moisture environment. The key molecular design was realized by a ring-opening reaction of a cyclic carbonate to introduce a pendant hydroxyl group four or five atoms away from an acyclic acetal repeat unit. In the presence of an acid catalyst, such a hydroxyl group allows an intramolecular transacetalization to form a more stable cyclic acetal and effectively cleave the polymer. A small molecule model containing the hydroxyurethane-acetal (HU-acetal) moiety was synthesized and confirmed by NMR to show the expected cyclization under an acidic, low moisture solvent environment. A step-wise polymerization of a diamine and a bis(cyclic carbonate)acetal monomer forms a linear, acid-degradable poly(HU-acetal) up to 50 kDa, while a diamine-terminated derivative of HU-acetal readily reacts with trimesoyl chloride in interfacial polymerization to form acid-degradable, oil-core polyamide microcapsules. Encapsulation of a hydrophobic photoacid generator (PAG) in the oil core of the microcapsules introduced photo-triggered degradation that saw the collapse of capsules shell and release of the liquid core oil in 30 minutes under exposure to 365 nm LED UV, thereby demonstrating the effectiveness of photoacid-triggered degradation of poly(HU-acetal) in a hydrophobic environment.

To my parents

In remembrance of my maternal grandmother

Acknowledgements

I would like to thank my advisor, Prof. Steven C. Zimmerman, for the opportunity to join his research team and receive scientific training under his tutelage, and for his patience, guidance, and faith in me as an aspiring chemist. I also want to thank my committee members, Prof. Paul V. Braun, Prof. Jianjun Cheng, and Prof. Nancy R. Sottos, for their constructive advice and for the chance to develop my intellectual skills at this world-renowned institution for chemistry research.

I also would like to express my gratitude towards several former senior members of Z-group: Dr. Chun Ho Wong, Dr. Dawn Ernenwein, Dr. Shampa Samanta, Dr. Yugang Bai, Dr. Gretchen Vincil, and Dr. Ying Li, who had encouraged me and taught me valuable knowledge and lessons, both in science and in life, throughout my time in the group. Those of us that joined the lab together in 2011, Dr. Long Luu, Dr. Lien Nguyen, Gary Suseno, Justin Wright and I shared a lot of common memory as we worked through the ups and downs of graduate school as classmates and labmates; I will surely remember both the fun and stressful times of our Z-group life and I want to thank you for all the support and encouragement that helped propel me through the challenges of grade school. Of course, I also want to thank all other current and past members of Z-group, particularly Brenda Andrade and Ephraim Morado who worked closely with me on the Dow project at various times, for making Z-group such a warm, cheerful, and supportive environment place to conduct my graduate research.

I want to thank my collaborators for their assistance on our projects, in particular Dr. Josh Grolman, Dr. Grant Hisao, Prof. Rienstra, my undergrads Nora Yanahan and Aoon Ravi, Kali Miller from the Braun group and the Dow scientists-Dr. Josh Katz, Dr. Keith Harris, and Dr.

Liang Chen. However, there are also many others with whom I have the privilege to work in the past six years, to list them all here will take too much space so I will just keep it simple: Thank you all, for you have directly or indirectly influenced and made me who I am today.

Lastly, I want to thank my parents for their never ending, unconditional love and support for me, no matter where I am and what I do.

Table of Contents

Chapter 1

General Introduction

This chapter aims to provide a concise overview of the concepts of encapsulation and pH-triggered release, with selective literature cited for reference.

Part of this chapter was adapted from the following publications:

1. Hsuan-Chin Wang, Yanfeng Zhang, Catherine M. Possanza, Steven C. Zimmerman, Jianjun Cheng, Jeffrey S. Moore, Keith Harris, and Joshua S. Katz*, Trigger Chemistries for Better Industrial Formulations, *ACS Appl. Mater. Interfaces*, **2015**, *7*, 6369-6382.
2. Hsuan-Chin Wang, Joshua M. Grolman, Aoon Rizvi, Grant S. Hisao, Chad M. Rienstra , and Steven C. Zimmerman*, pH-Triggered Release from Polyamide Microcapsules Prepared by Interfacial Polymerization of a Simple Diester Monomer, *ACS Macro Lett.*, **2017**, *6*, 321-325.

1.1 Encapsulation and pH-triggered release

Modern innovation in technology has been rapidly accelerating in large part as a result of advancement in chemical and materials sciences. From more effective drug formulations[1] to energy efficient electronic reader technology[2], the successes of many modern day products benefit directly or indirectly from high performance chemicals and materials. To ensure maximum performance of functional chemical species, which are often referred to as active ingredients or simply actives, encapsulation using cleverly designed excipient materials is a highly sought after strategy to protect and/or render the actives effective for the targeted applications. A typical encapsulation strategy aims to shield the encapsulated actives from damaging environments and minimize unintended actions that could lead to toxicity or contamination, which, in real world practice, translate directly to safer, more economical, and/or more efficient products because less material is needed to achieve the same or better performance with minimal adverse effects.[3]

In many applications such as drug delivery and pesticide dissemination, a part of the strategy for encapsulation of actives requires methods to effect the release of the active from its encapsulated state at the desired location and time of action. One such method is the employment of triggers to induce chemical, physical, or a mixture of chemical and physical changes to the encapsulant materials upon a specific stimulus to facilitate release of otherwise immobilized active ingredients. Significant academic research efforts and associated dollars have been spent on development of triggered-release chemistries and applications, though little has translated for industrial use.[4] To address this challenge, The Dow Chemical Company, the Zimmerman lab, and several other research groups at University of Illinois initiated a joint collaboration to explore novel trigger release and encapsulant chemistries, mechanisms, and systems. Our efforts to develop new triggerable polymeric encapsulants focused on the use of pH as a trigger because the ubiquity of environments with specific pH levels in various application areas ranging from biomedical to agricultural to those in consumer products and industrial processes.[5-7]

The most common chemical strategies for using pH change as a trigger generally fall into two categories: acid/base-catalyzed covalent bond cleavages and hydrophilicity/phobicity changes by variation in protonation states. The use of the most common types of acid-labile covalent bonds including acetals, orthoesters, imines, hydrazones, and esters in degradable polymers has been recently reviewed by Binauld and Stenzel.[5] The cleavage of acid-labile bonds in an encapsulating material can lead to structure fragmentation, depolymerization, or polarity change, translating to enhanced permeation and release of encapsulated cargo.[8-10] In the cases of cationic and anionic polymeric encapsulants, variations in pH alter the degree of ionization through protonation or deprotonation, leading to changes in electrostatic interactions and hydrophilicity. A ketal-containing cationic poly(β-aminoester) nanoparticle developed by Almutairi and co-workers

demonstrates an interesting application of both acid-catalyzed bond cleavage and acid-induced change in protonation state.[8] Prepared from a copolymer of ketal and aminoester monomers, the nanoparticles exhibit a burst release profile in acidic media. The swelling effect from secondary amine protonation enhances the uptake of acidic water, resulting in accelerated ketal cleavage throughout the nanoparticles. Aminals, amine analogues of the oxygen-based acetal structures, are less commonly encountered in synthetic soft materials compared to acetals, most likely because of relatively lower stability. However, for a special type of cyclic aminal structure, 1,3,5-triazaadamantanes (TAA), the stability is substantially higher owing to their three-dimensional, diamond-like structure. Synthesized by a condensation of a 1,1,1-tris(aminomethyl) compound with three aldehydes, TAAs are tuned by substituent effects to degrade at different rates and have been derivatized by Zimmerman and co-workers for use in acid-responsive materials such as hydrogels and dendritic structures.[11-13]

Compared to acid-triggered release, which has dominated the current literature largely as a result of strong interest in drug delivery research, base-triggered release has received relatively less attention and is most often realized by anionic polymeric encapsulants.[14] Under a higher pH environment, anionic polymers such as those based on polyacrylic acids, undergo ionization through increased deprotonation, causing the encapsulants to swell or disintegrate.[15,16] Polymers that utilize base-mediated or catalyzed covalent bond degradation have also been reported, many of which have shown promise to be developed for triggered release applications.[17–20] Finally, degradable polymeric encapsulants capable of incorporating a variety of triggers, such as base, acid, or light, through a modular synthetic approach, has recently been reported.[21,22]

1.2 References

(1) Mitragotri, S.; Burke, P. A.; Langer, R. *Nat. Rev. Drug. Discov.* **2014**, *13*, 655.

(2) Comiskey, B.; Albert, J. D.; Yoshizawa, H.; Jacobson, J. *Nature* **1998**, *394*, 253.

(3) Andrade, B.; Song, Z.; Li, J.; Zimmerman, S. C.; Cheng, J.; Moore, J. S.; Harris, K.; Katz, J. S. *ACS Appl. Mat. & Interfaces* **2015**, *7*, 6359.

(4) Fleige, E.; Quadir, M. A.; Haag, R. *Adv. Drug Deliv. Rev.* **2012**, *64*, 866.

(5) Binauld, S.; Stenzel, M. H. *Chem. Commun.* **2013**, *49*, 2082.

(6) Herrmann, A. *Angew. Chem. Int. Ed.* **2007**, *46*, 5836.

(7) Wang, H.-C.; Zhang, Y.; Possanza, C. M.; Zimmerman, S. C.; Cheng, J.; Moore, J. S.; Harris, K.; Katz, J. S. *ACS Appl. Mater. & Interfaces* **2015**, *7*, 6369.

(8) Sankaranarayanan, J.; Mahmoud, E. A.; Kim, G.; Morachis, J. M.; Almutairi, A. *ACS Nano* **2010**, *4*, 5930.

(9) Garripelli, V. K.; Kim, J. K.; Namgung, R.; Kim, W. J.; Repka, M. A.; Jo, S. *Acta Biomater.* **2010**, *6*, 477.

(10) Klaikherd, A.; Nagamani, C.; Thayumanavan, S. *J. Am. Chem. Soc.* **2009**, *131*, 4830.

(11) Balija, A. M.; Kohman, R. E.; Zimmerman, S. C. *Angew. Chem. Int. Ed.* **2008**, *47*, 8072.

(12) Kohman, R. E.; Zimmerman, S. C. *Chem. Commun.* **2009**, 794.

(13) Kohman, R. E.; Cha, C.; Zimmerman, S. C.; Kong, H. *Soft Matter* **2010**, *6*, 2150.

(14) Oerlemans, C.; Bult, W.; Bos, M.; Storm, G.; Nijsen, J. F. W.; Hennink, W. E. *Pharmaceutical Research* **2010**, *27*, 2569.

(15) Brannon-Peppas, L.; Peppas, N. A. *J. Control. Release* **1989**, *8*, 267.

(16) Feng, N.; Dong, J.; Han, G.; Wang, G. *Macromol. Rapid Commun.* **2014**, *35*, 721.

(17) De Geest, B. G.; Van Camp, W.; Du Prez, F. E.; De Smedt, S. C.; Demeester, J.; Hennink, W. E. *Macromol. Rapid Commun.* **2008**, *29*, 1111.

(18) Possanza Casey, C. M.; Moore, J. S. *ACS Macro Lett.* **2016**, *5*, 1257.

(19) Darensbourg, D. J.; Wei, S.-H. *Macromolecules* **2012**, *45*, 5916.

(20) Li, C.; Sablong, R. J.; van Benthem, R. A. T. M.; Koning, C. E. *ACS Macro Letters* **2017**, *6*, 684.

(21) Esser-Kahn, A. P.; Sottos, N. R.; White, S. R.; Moore, J. S. *J. Am. Chem. Soc.* **2010**, *132*, 10266.

(22) Zhang, Y.; Ma, L.; Deng, X.; Cheng, J. *Polym. Chem.* **2013**, *4*, 224.

Chapter 2

Multi-pH-triggerable polyamide microcapsules

Part of this chapter was adapted from the following publications:

1. Hsuan-Chin Wang, Yanfeng Zhang, Catherine M. Possanza, Steven C. Zimmerman, Jianjun Cheng, Jeffrey S. Moore, Keith Harris, and Joshua S. Katz*, Trigger Chemistries for Better Industrial Formulations, *ACS Appl. Mater. Interfaces*, **2015**, *7*, 6369-6382.
2. Hsuan-Chin Wang, Joshua M. Grolman, Aoon Rizvi, Grant S. Hisao, Chad M. Rienstra , and Steven C. Zimmerman*, pH-Triggered Release from Polyamide Microcapsules Prepared by Interfacial Polymerization of a Simple Diester Monomer, *ACS Macro Lett.*, **2017**, *6*, 321-325.

2.1 Introduction

Thin-shell encapsulation is attractive because the large core-to-shell volume-ratio enables delivery of a large payload with minimal investment in the material for the surrounding shell. However, for many applications, a high carrying capacity is insufficient by itself; an efficient, stimuli-responsive release mechanism is required to achieve both the desired release rate and a high payload delivery. Not surprisingly, pH is a popular and useful release trigger for thin-shell capsules given the ubiquity of water with specific pH levels in various application environments.[1-3]

Most current encapsulants that are triggered by a pH stimulus utilize either low or high pH to initiate efficient payload release.[4-11] A unique type of pH responsive materials is polyampholytes, which can respond to both high and low pH by virtue of their polymeric framework containing both cationic and anionic groups. Stimuli-responsive polyampholytes have been used in gels, films, and thin-shell capsules[12-18], the latter typically formed around a template or at a liquid-liquid interface. However, as is common for polyelectrolyte assemblies, preparation of stable, liquid-core-thin-shell ampholyte capsules generally requires multiple steps such as layer by layer

deposition, core template dissolution, shell crosslinking for structural stabilization or cargo encapsulation by post-fabrication loading. Furthermore, although dual acid/base-triggered release of small molecules from polyampholyte hydrogels and thin films have been reported, analogous release from liquid-core microcapsules, to the best of our knowledge, has yet to be demonstrated.[19,20] In this work, we fabricated in one step a high capacity polymeric microcapsule that remained stable in a non-polar environment, but demonstrated sustained release of a small molecule dye at neutral pH and accelerated release at both acidic and basic pH.

2.2 Goals and approaches

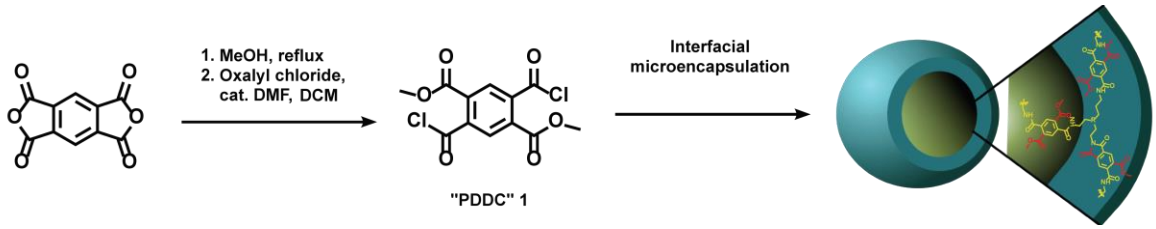

Scheme 2.1. Syntheses of terephthalyol chloride monomer **1** and base-labile microcapsules.

To develop a pH-responsive polymeric encapsulant, we utilized pyromellitic diester diacid chloride **1** (PDDC) as a pH-degradable monomer (**Scheme 2.1**). PDDC contains four carbonyl groups at the 1, 2, 4, and 5 positions that provide a highly electron-withdrawing effect on the structure, which is evidenced by the significantly lower 1st pKa of ~ 2 for the corresponding carboxylic acid compared to that of benzoic acid at ~ 4. Such an effect renders PDDC susceptible to hydrolysis and could serve as the responsive component in a pH-degradable polymer.

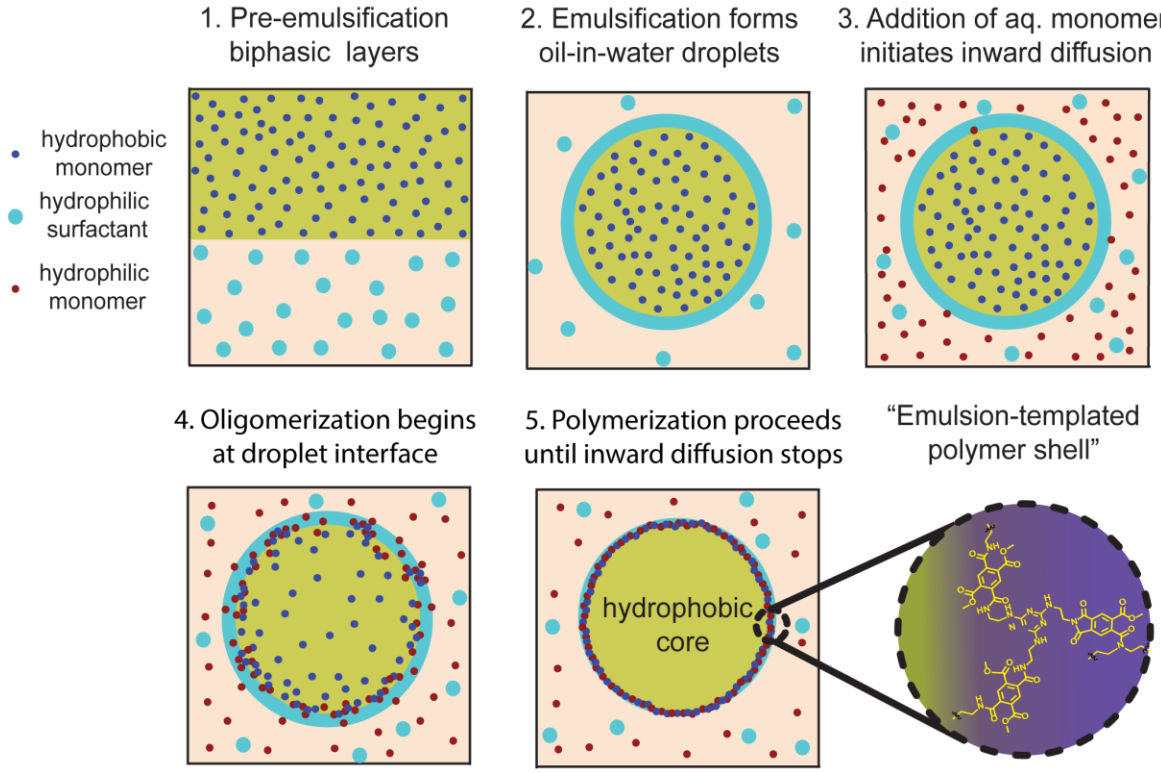

Figure 2.1. Stepwise illustrations of interfacial microencapsulation; green color represents a hydrophobic solvent and light pink color represents water.

To prepare robust, high capacity microcapsules, we utilized interfacial microencapsulation, a demonstrated technique extensively investigated and, indeed, regularly employed on an industrial production level.[21,22] Analogous in concept to the classic "nylon-rope trick",[23] interfacial polyamide microencapsulation takes advantage of the rapid polymerization of a hydrophobic polyacid chloride with hydrophilic polyamines at the interface of immiscible phases to ensure the full encapsulation of the emulsified O/W or W/O droplet template. A step-wise illustration of interfacial microencapsulation is detailed in **Figure 2.1**. Our proposed design has the advantages of ease of synthesis, structural simplicity, and utilization of a mature microencapsulation technology, all of which may translate to lower cost and accelerated commercialization. We intend to investigate 1) if the polyamides demonstrate suitable barrier

properties and structural integrity, and 2) if pH-dependent polymer degradation and triggered release could be demonstrated and tuned by modifying the chemical structures.

2.3 Optimization of microcapsule synthetic conditions

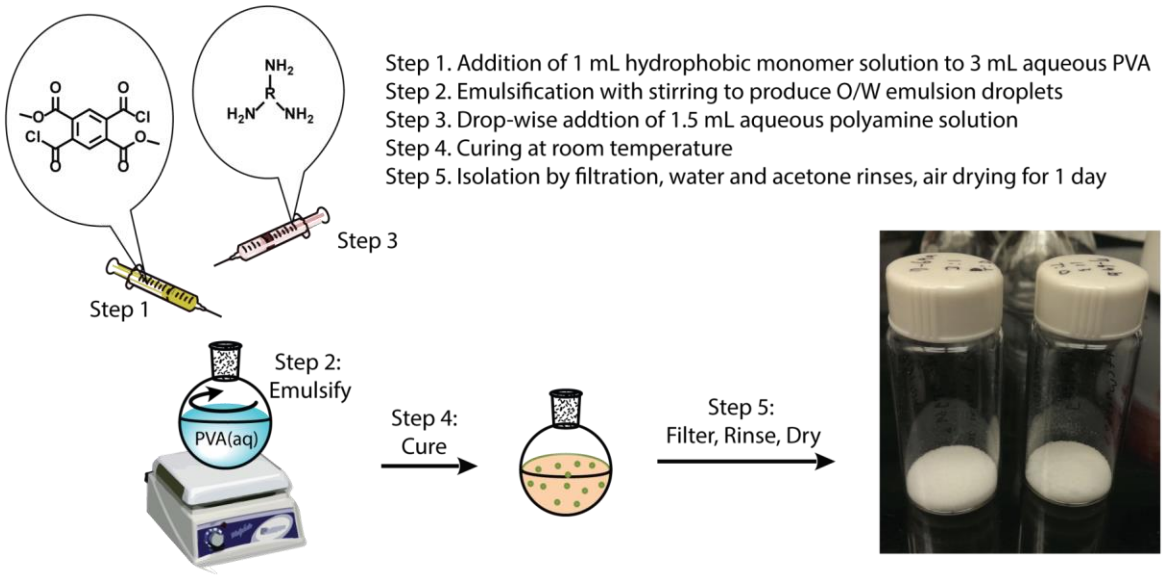

Figure 2.2. Illustrations of microcapsule synthesis with polyamine and PDDC.

The ability to retain cargo of interest under the desired storage condition is a key prerequisite in the development of an effective encapsulant. Therefore, preliminary efforts focused on identifying polyamines that form stable, high quality microcapsules. The quality of microcapsules were assessed by 1) encapsulation efficiency of the core hydrophobic phase as determined by mass recovery, and 2) morphology of collected capsules (i.e., free flowing powders or aggregated solids). Capsules were synthesized, as shown in **Figure 2.2**, using a modified literature procedure[8] that has been shown to produce stable polyamide microcapsules using diethylenetriamine (DETA) and trimesoyl chloride (TMC) as monomers.

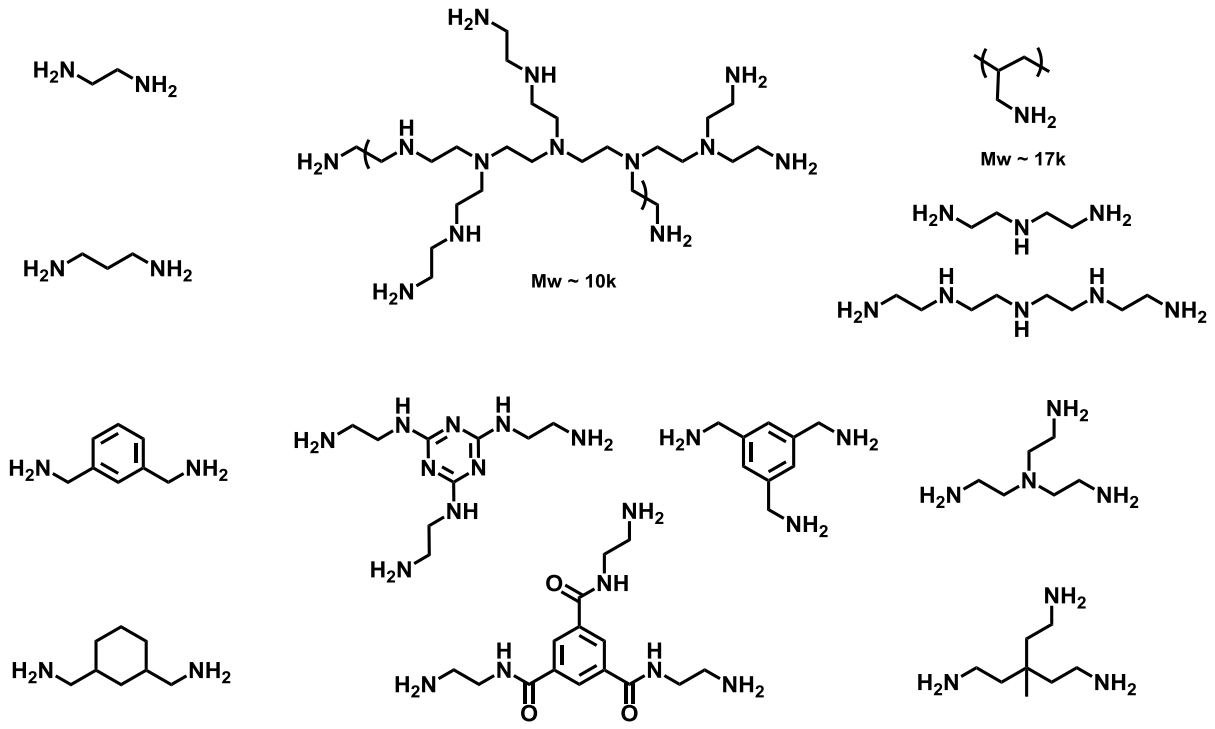

Figure 2.3. Polyamines screened for PDDC microcapsules synthesis.

Several commercially available water-soluble polyamines (**Figure 2.3**) were screened using the same set of synthetic parameters with toluene as the hydrophobic core solvent. Initial polymerization attempts with commercially available diamines such as ethylene diamine, 1,3-diaminopropane, *m*-xylylenediamine, and 1,3-bis(aminomethyl)cyclohexane afforded polymeric shells that failed to retain the core solvent. The observed rapid leakage was likely due to a lack of crosslinking in the linear polyamides produced. Diethylenetriamine (DETA), which is capable of forming a crosslinking point at its secondary amine, produced soft, aggregated microcapsules with improved core solvent retention of ca. 30%, despite the fact that DETA is known to polymerize interfacially with the structurally analogous terephthaloyl chloride (TC) to form polyamide microcapsules with good barrier properties.[24] A plausible hypothesis to explain the observed differences in barrier and mechanical properties is a reduced level of cross-linking at

the secondary amine of DETA as a result of steric hindrance from the ester groups in the ortho-position. To see if better barrier through enhanced crosslinking could be achieved by employing a tris-type primary amine crosslinker, tris(aminoethyl)amine, TAEA, was tested. TAEA is essentially a more extended version of DETA with three chemically equivalent primary amines that was expected to crosslink with PDDC more efficiently than DETA. Microencapsulation using PDDC and TAEA afforded microcapsules that were resistant to aggregation and demonstrated encapsulation efficiency up to 94%.

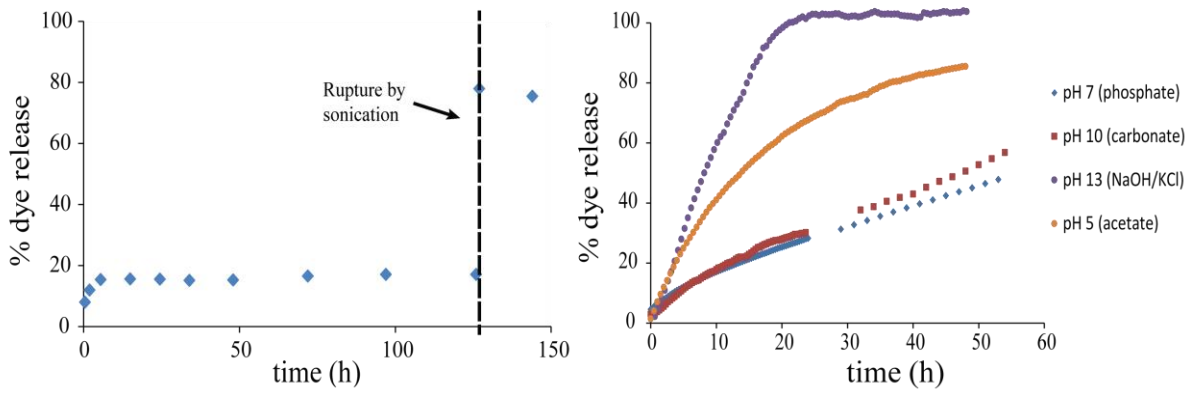

Figure 2.4. a) dye release from TAEA microcapsules incubated in toluene. b) Dye release from TAEA microcapsules suspended between toluene and an aqueous pH buffer.

In order to assess the permeability of the shell to the toluene core solvent and to check for defects in the capsule shell wall, TAEA capsules were synthesized with a toluene solution containing coumarin 1 dye and incubated in toluene. As seen in **Figure 2.4a**, TAEA capsules showed rapid equilibration to ~ 15% release and remained stable until capsules were broken by sonication to reach a final release of ca. 75%, suggesting the TAEA microcapsules were capable of retaining at least the majority of the initially added dye.

To investigate pH dependence of release, TAEA capsules loaded with coumarin 1-containing toluene cores were subjected to pH 5 (0.1 M acetate), pH 7.4 (0.1 M phosphate), pH 10 (0.1 M carbonate), and pH 13 (0.2 M NaOH/KCl) buffers to assess the effects of pH on the release rate of the encapsulated dye. **Figure 2.4b** shows the percent dye released as a function of incubation time at various pH values. At pH 13, the most rapid release was observed, reaching around 100% in less than 20 h and remained stable thereafter. At pH 10 and 7.4, the release rate were slower than at pH 13 but interestingly were quite similar; both reached around 30% by t = 20 h and continued with an almost identical release profiles. The rate of dye release at pH 5 was significantly faster than at pH 7.4 and 10, exceeding 60% in 20 h. The observed release profiles at these pH values indicated that coumarin 1 dye release from TAEA capsule was not necessarily faster at a higher pH. The observed release behavior at different pH values could be explained by the structure of the crosslinked polymer shell. In addition to the anionic carboxylate groups formed under basic hydrolysis, cationic tertiary amine groups from the TAEA monomer are also present in the polymer, meaning that an increase or decrease in pH could lead to enhanced swelling due to increased electrostatic repulsions between polymer chains.

While TAEA proved to be an effective trisamine crosslinker for microencapsulation, the lack of differentiable stability between pH 7 and 10 environments prompted us to test additional polyamine crosslinkers. Commercially available oligomeric and polymeric amines such as branched polyimine and polyallylamine yielded capsules with poor morphologies and little retention of core solvent. To further screen for a suitable crosslinker, four literature known trisamine crosslinkers **2**, **3**, **4** and **5** were selected for their relative ease of syntheses as well as potential to provide good barrier properties (**Scheme 2.2**).

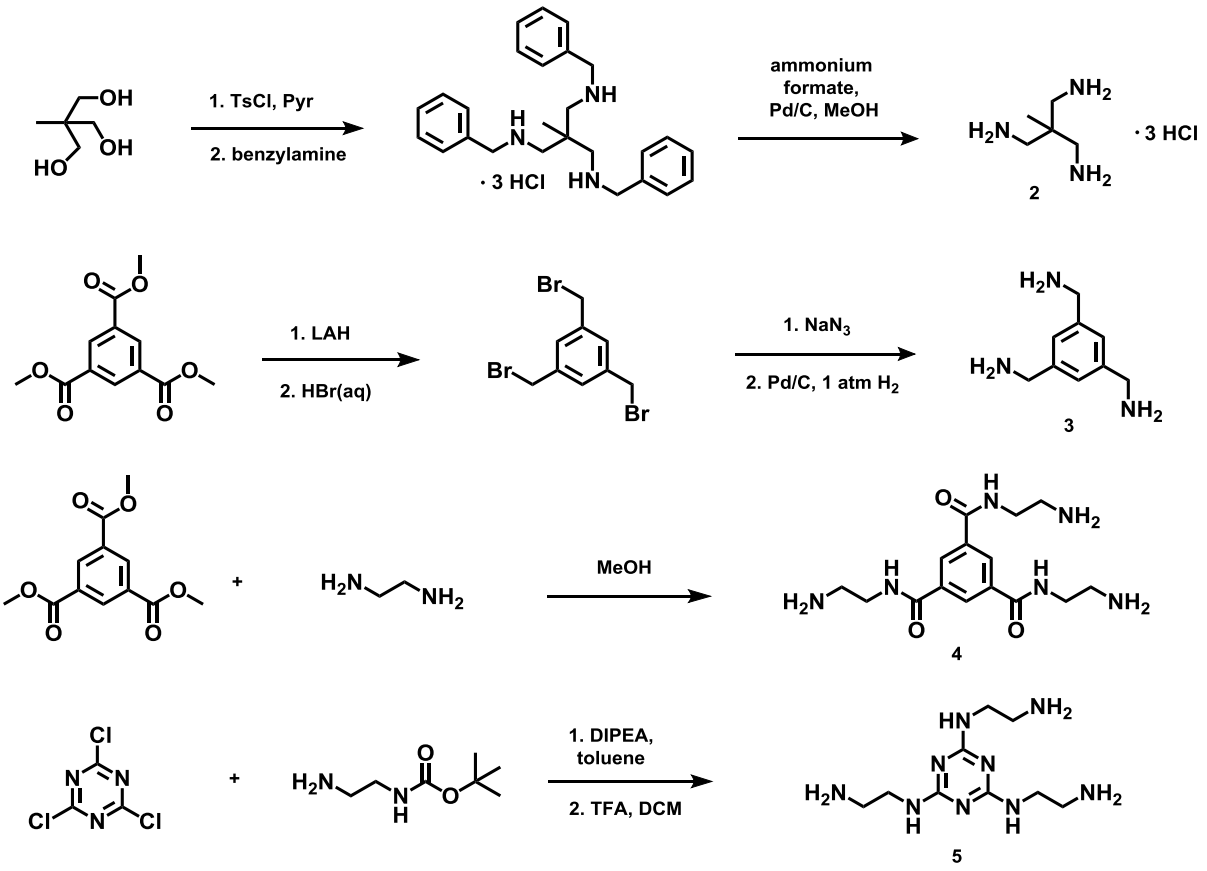

Scheme 2.2. Syntheses of trisamine crosslinkers **2**, **3**, **4,** and **5.**

Tris(aminomethyl)ethane **2**, is an alkyl acyclic crosslinker that could serve as a smaller, tertiary amine-free analogue of TAEA. The three-step synthesis yielded **2** as a trihydrochloride salt. Microencapsulation was attempted using a solution of **2** in 0.1 M pH 10 carbonate buffer. The formed polymer capsules did not survive purification and collapsed to into white solid residues. It should be noted, though, a higher pH buffer would have allowed a higher concentration of free amine in **2** to be available for polymerization and possibly led to a faster, more complete shell formation that would afford a more robust microcapsule. Because of lack of success with alkyl based crosslinkers, a series of primary amine crosslinkers bearing aromatic rings were synthesized to see if enhanced barrier could be achieved with bulky ring structures. 1,3,5-tris(aminomethyl)benzene **3** was prepared from catalytic hydrogenation of 1,3,5-

tris(azidomethyl)benzene, which was synthesized in three steps starting with a one-pot reduction and bromination of trimethyl 1,3,5-benzencarboxylate with $LiAlH_4$ and hydrobromic acid and subsequent azidation of the 1,3,5-tris(bromomethyl)benzene product with NaN_3. Interfacial polymerization of trisamine **3** with **1** resulted in capsules that were highly permeable to water miscible organic solvents such as acetone, methanol, and THF. Visible swelling of the capsules accompanied loss of the toluene core solvent, leading to near complete release and capsule mass loss during the purification step. Tris(2-aminoethyl)-1,3,5-benzenetricarboxylamide **4** was synthesized according to literature[25] and utilized for capsules making. Although the presence of three amide groups could enhance physical crosslinking by hydrogen bonding, the resulting microcapsules aggregated and collapsed during the filtration step.

The last aromatic crosslinker tested was the triazine type trisamine **5** that was synthesized by refluxing mono *N*-Boc-protected ethylenediamine with cyanuric chloride in toluene and subsequently removing the Boc group using trifluoroacetic acid. The triazine **5** was selected because of its resemblance to melamine-formaldehyde based polymer, which has been used successfully in the production of stable microcapsules. Polymerization produced microcapsules with high mass recovery (70 – 83%) but aggregation upon drying prevented their isolation in dry powder form. To further confirm encapsulation efficiency while bypassing the issue of aggregation, the melamine-type microcapsules were rinsed to remove excess trisamine monomer and, without drying, immediately suspended between an aqueous pH buffer and toluene to monitor dye release. At pH 10, the release rate was significantly faster than at pH 7.4, while at pH 5 the rate was slightly higher. Sodium hydroxide solution (1M) was used to accelerate degradation of capsules for faster release (**Figure 2.5**). In all cases, an immediate jump in the release rates was observed and after 144 h, the release percentages all began to plateau and

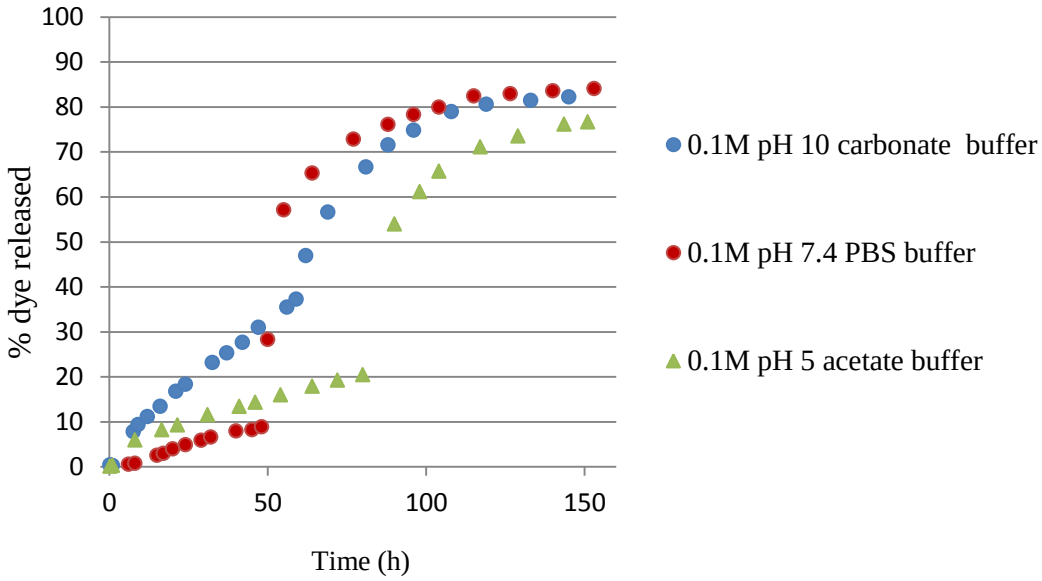

Figure 2.5. Dye release from triazine **5**-PDDC microcapsules in contact with aqueous buffers of various pH values.

converged at approximately 80%, which matched the mass recovery values obtained from previous experiments with triazine **5**. The issue of capsule aggregation upon drying was resolved when a mixture of triazine **5**/DETA solution was used for polymerization. Molar ratios ranging from 1:3 to 3:1 triazine **5**: DETA afforded fine, free-flowing white powders with mass recovery of 80-90%, suggesting highly effective encapsulation. Subsequent work focused on optimization of microcapsule synthesis. Various parameters such as reaction time and monomer concentrations were adjusted in series of experiments, and it was found that the concentration of the PDDC monomer, the duration of reaction, and the volume ratio between the surfactant and the organic phase are crucial to obtaining good quality capsules. Specifically, a saturated toluene solution (30 mg/mL), a reaction time of 60 min, and a volume ratio of 3:1 aqueous polyvinyl alcohol surfactant to PDDC in toluene yielded toluene-loaded microcapsules with spherical morphologies, high mass recoveries, and good dispersability in the form of a dry, free flowing powder after purification.

2.4 Characterization of triazine:DETA microcapsules

In addition to optical microscopy that was used for preliminary visual assessment of microcapsules, scanning electron microscopy (SEM) provided detailed morphological analyses that confirmed the majority of microcapsules had diameters between 200 and 350 µm (**Figure 2.6a & c**) and possessed a rough inner shell surface, an observation consistent with literature precedents.[26,27] Shell thicknesses were found to be between 0.7 to 1.5 µm based on cross-sectional SEM images (**Figure 2.6b & d**). The dimensional variations found in the microcapsules reflected the size range of emulsified droplet templates. The inner and outer surfaces also differed in their roughness, with the outer surface smoother than the inner surface,

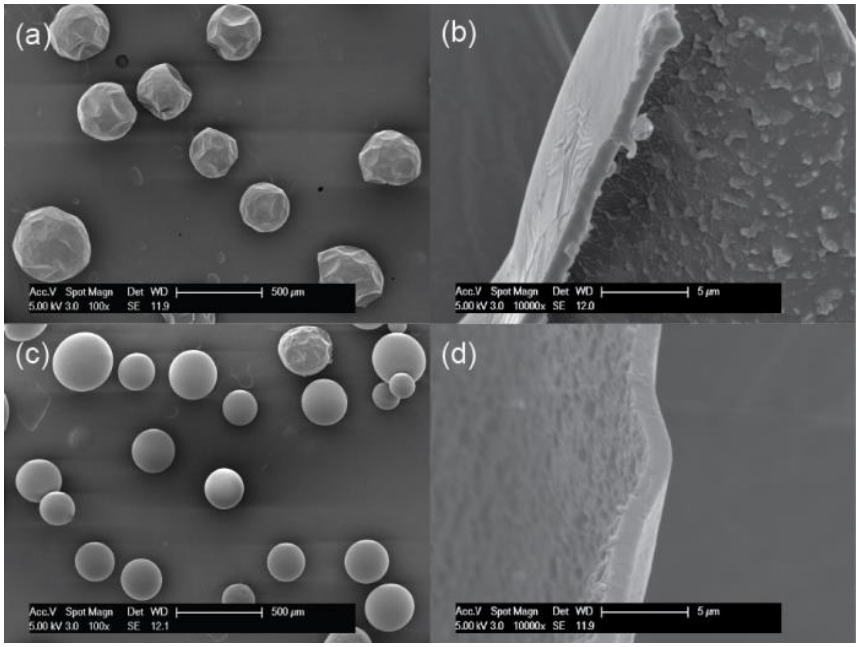

Figure 2.6. SEM images of a) 3:1 triazine **5**:DETA, b) cross-section of 3:1 triazine **5**:DETA capsule shell, c) 1:1 triazine **5**:DETA capsules, d) cross-section of 1:1 triazine **5**:DETA capsule shell. Scale bars: a) and c) 500 µm; b) 5 µm; d) 2 µm.

which were lined with small pillar-like features. The rugged inner surface is characteristic of interfacially polymerized microcapsules and is thought to be evidence for the inward, self-limiting diffusion of the amine monomers toward the hydrophobic core center.[26]

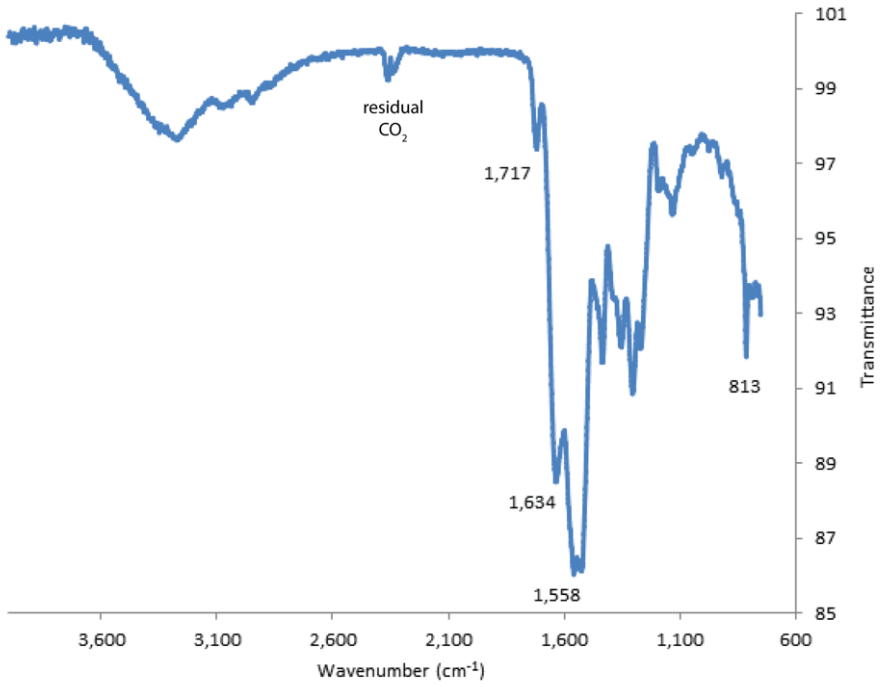

Figure 2.7. ATR FT-IR spectrum of dried polymer shell.

Chemical composition of the polymer shell was analyzed using solid state attenuated total reflectance FT-IR (ATR FT-IR) because the highly cross-linked polymer shell prevented dissolution in common solvents for solution state analysis. As seen in **Figure 2.7**, ATR FT-IR spectroscopy confirmed the presence of amide (characteristic amide I at 1634 cm^{-1}, amide II at ~1557 cm^{-1} likely overlapping with C-N band from the triazine) and the inclusion of triazine moieties (813 cm^{-1}, ring out of plane deformation)[27] in the polymer shell. The peak ca. 1716 cm^{-1} is likely the carbonyl stretch of remaining ester or imide, the latter could form in an intramolecular cyclization of the ortho amide-ester moiety. Although differentiation of these two possible functional groups was difficult, we were able to experimentally confirm that both groups readily hydrolyze at high pH using small molecule analogs (see Section 2.6 on investigation on potential degradation mechanisms) and therefore expected both structures to lead to the anticipated pH response. While the incorporation of DETA monomer was difficult to

characterize and quantify because of its similarity to the alkyl portion of the triazine **5**, we have shown that addition of a suitable amount of DETA to the triazine **5** solution enhanced capsule barrier properties and yielded capsules that did not aggregate upon drying. While the exact role of DETA's secondary amine remained unclear, its importance in enhancing the barrier properties of the microcapsules was demonstrated by control experiments in which analogous mole ratios of 1,5-diaminopentane were mixed with triazine **5** to prepare PDDC microcapsules that rapidly lost their core solvent after 1 h of air drying (**Figure 2.8**).

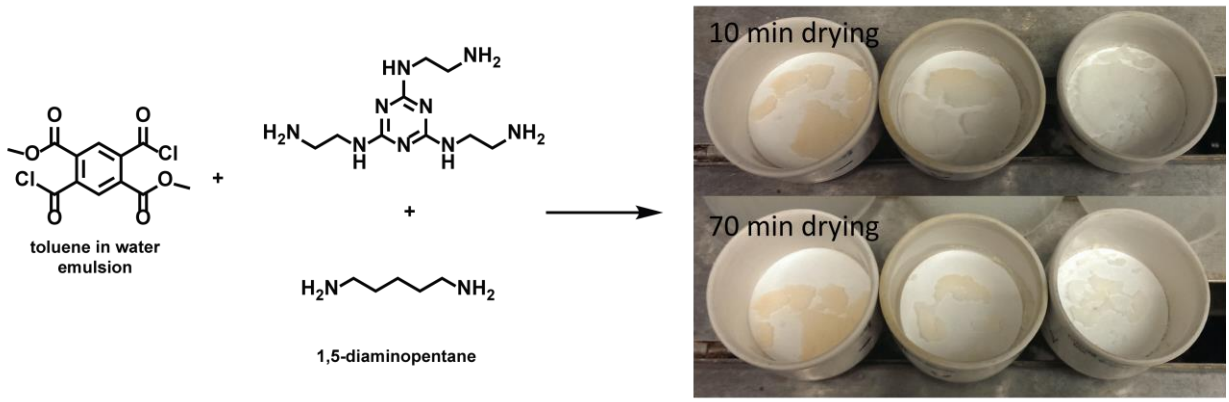

Figure 2.8. Control experiments using 1,5-aminopentane as a "secondary amine-free" analog of DETA. Microcapsules collapsed and lost majority of core solvent after 1 h of air drying after purification.

The thermal stability of PDDC microcapsules prepared from triazine **5** and DETA was evaluated by thermal gravimetric analysis (TGA), which measures the weight loss from microcapsules in a specified temperature range and thus provides insight into how well the microcapsules retain its core material up to a preset temperature. In the TGA experiment involving toluene-loaded 1:1 triazine **5**:DETA microcapsules, a temperature range from 20 to 300 ^{o}C was selected and the temperature was set to ramp at a rate of 5 ^{o}C /min. As indicated by **Figure 2.9**, clearly observable onset of microcapsules weight loss of 4% initiated at around 130 ^{o}C but a significant drop of ca. 85% total weight only occurred between 180 and 195 ^{o}C. The

high temperature of weight loss demonstrated that the microcapsules were able to retain majority of the encapsulated toluene at temperatures significantly above the boiling point of toluene (110 ^{o}C at ambient pressure) and suggested that polymer shell provides a robust barrier against leakage of toluene vapor. Similar observation of superheating toluene-loaded microcapsules to above boiling point of toluene has also been reported in literature.[28]

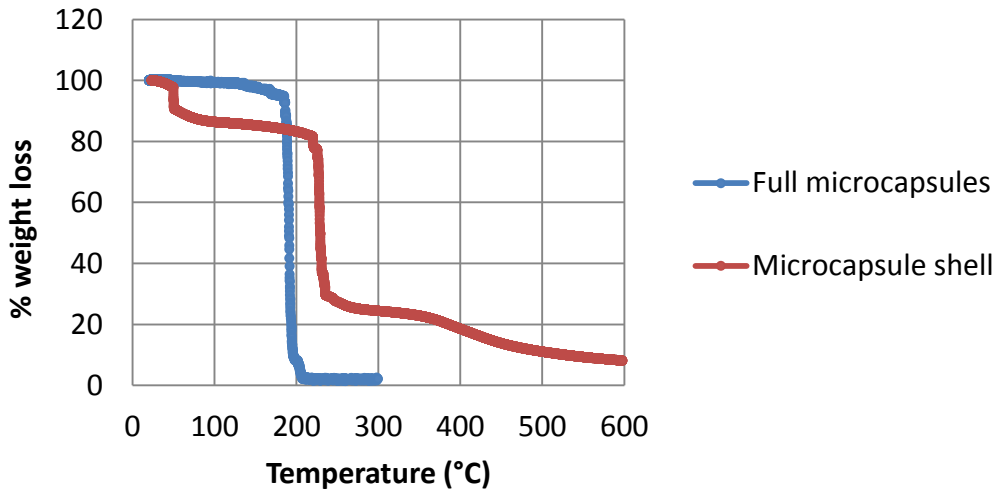

Figure 2.9. TGA of PDDC microcapsules prepared from 1:1 triazine **5**:DETA (Blue) and shredded microcapsules shell polymer (Red).

It is also worth noting that the ~ 90% weight loss correlated well with the core weight percentages of encapsulated toluene that were experimentally determined by shredding microcapsules with sonication and obtaining the weight difference between the initial total weight of the microcapsules and the shredded dried polymer shell. The TGA of shell polymer indicated significant weight loss occurred at ~ 220 ^{o}C, suggesting the large weight loss at 180 ^{o}C observed in the TGA of full microcapsules was not entirely a result of polymer degradation. The initial weight loss at around 50 ^{o}C was likely caused by residual rinse solvents as acetone, methanol and diethyl ether were used to rinse the shredded shell polymer during filtration.

2.5 Barrier properties and pH-dependent release of a model dye

To assess barrier properties and responsiveness to pH triggers, coumarin 1-loaded PDDC microcapsules prepared from a 1:1 triazine **5** : DETA were incubated in toluene with and without aqueous pH buffers. Identical experiments involving dye-loaded 1:1 triazine **5**:DETA microcapsules prepared from terephthaloyl chloride (TC) served as controls to verify the effect of PDDC. The concentration of released coumarin 1 dye was monitored in the toluene layer by UV-Vis spectrometry (**Figures 2.10a & b, 2.11a**). In both PDDC and TC microcapsules,

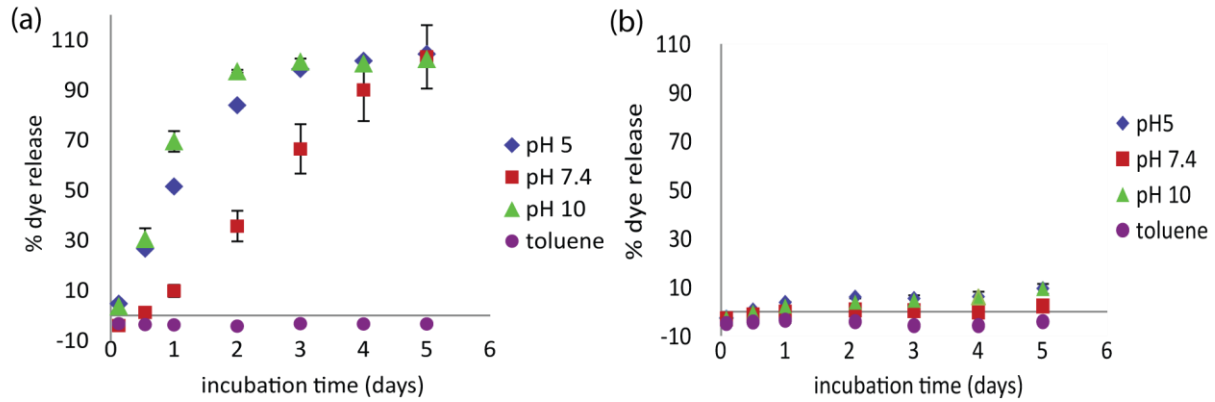

Figure 2.10. Coumarin 1 dye release from a) 1:1 triazine **5**:DETA/PDDC microcapsules, and b) 1:1 triazine **5**:DETA/TC microcapsules (control), under different solvent environments.

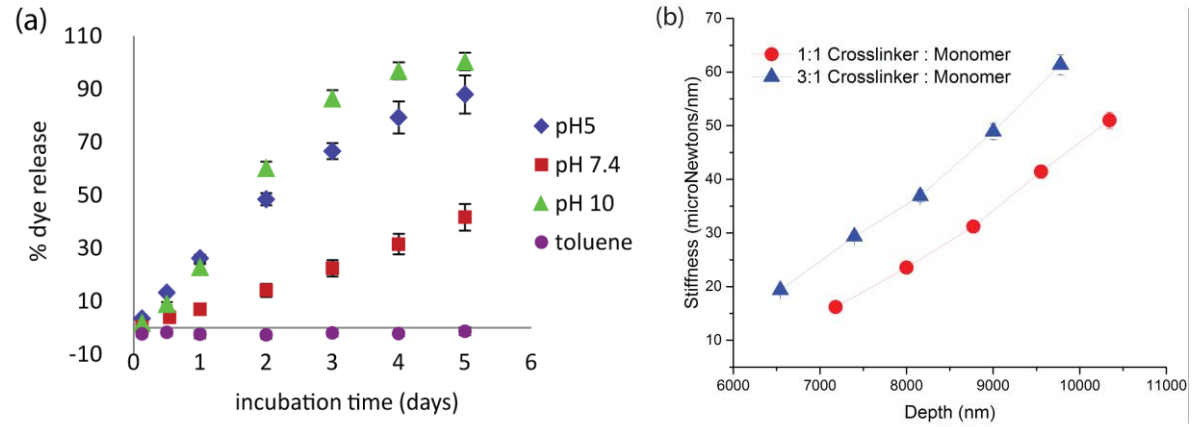

Figure 2.11. a) Coumarin 1 dye release from 3:1 triazine **5**:DETA/PDDC microcapsules; b) Stiffness measurements by nanoindentation on 1:1 and 3:1 triazine **5**:DETA/PDDC microcapsules.

stability in toluene over the course of at least 5 days was confirmed by the absence of detectable concentration of coumarin 1 dye in the toluene supernatant. Control experiments with TC microcapsules (**Figure 2.10b**) showed little to no response to toluene or pH buffers. However, in samples of PDDC microcapsules prepared from 1:1 triazine **5** :DETA that were incubated between aqueous 0.1 M pH buffers and toluene, dye release was observed, although with an unexpected trend: at pH 5 and pH 10, a similar first-order like release profile was detected, whereas at pH 7, a more suppressed, linear release was observed (**Figure 2.10a**).

Similar trend was also seen in capsules prepared with a higher amount of triazine crosslinker monomer (3:1 monomer ratio), although the release rates were visibly suppressed across all three pH values tested (**Figure 2.11a**). The reduced release rates likely resulted from an increased degree of crosslinking in the polymer shell, which in theory would slow diffusion and increase resistance to hydrolysis. Stiffness measurements using nanoindentation indicated increased stiffness in microcapsules with 3:1 triazine **5**:DETA compared to ones synthesized from 1:1 triazine **5** :DETA (**Figure 2.11b**), providing evidence for increased crosslinking in the 3:1 triazine **5** :DETA microcapsules.

2.6 Investigation into possible release mechanisms

To explain the barrier properties of the PDDC microcapsules observed in nonpolar and various pH environments, we proposed two mechanistic hypotheses: 1) The PDDC microcapsules are susceptible to hydrolysis under both basic and weakly acidic conditions, leading to relatively large swelling of the microcapsules at pH 5 and pH 10, and 2) presence of residual unreacted amines from the aqueous monomers leads to the formation of a polycationic shell that protonates and swells under an acidic condition.

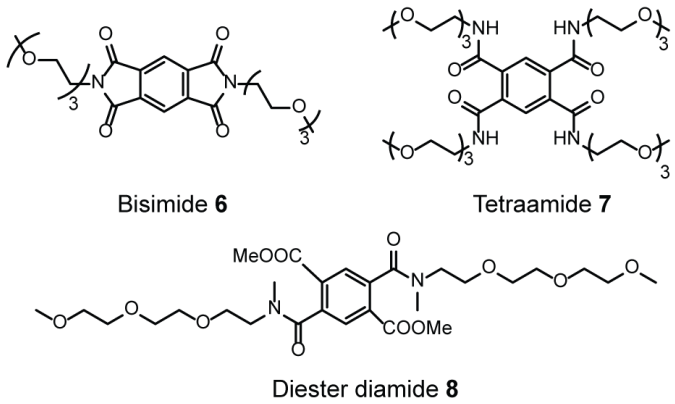

Figure 2.12. Small molecule analogs to simulate potential microcapsule shell polymer structures.

To investigate whether the observed release trends were controlled by ester or imide hydrolysis, three structurally analogous small molecules (bisimide **6**, tetraamide **7**, and diester diamide **8**, shown in **Figure 2.12**) were dissolved in D_2O at pD 5, 7, and 10 and their degradation kinetics monitored by ^1H NMR. As **Figures 2.13, 2.14, and 2.15** indicated, all three molecules were significantly more stable at pD 5 than at pD 7 and pD 10. The bisimide and diester diamide analogs remained largely unchanged in pH 5 but hydrolyzed at increased rates as the pH increased to 7 and 10. The stability observed at pH 5 suggested the weak acid hydrolysis mechanism was unlikely a major contributor to the relatively fast release. These data are consistent with operation of the originally designed mechanism in which protonation of residual, unreacted amine groups increased swelling as a result of the increased polyionic character. Compared to TC, the structurally hindered PDDC potentially prevented the amine groups from completely reacting with the acid chloride groups, effectively rendering the capsule shell "cationic" when exposed to low pH.

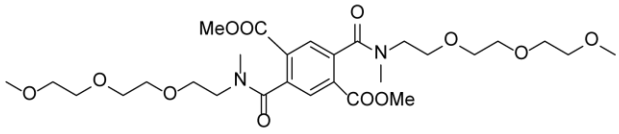

Diester diamide **8**

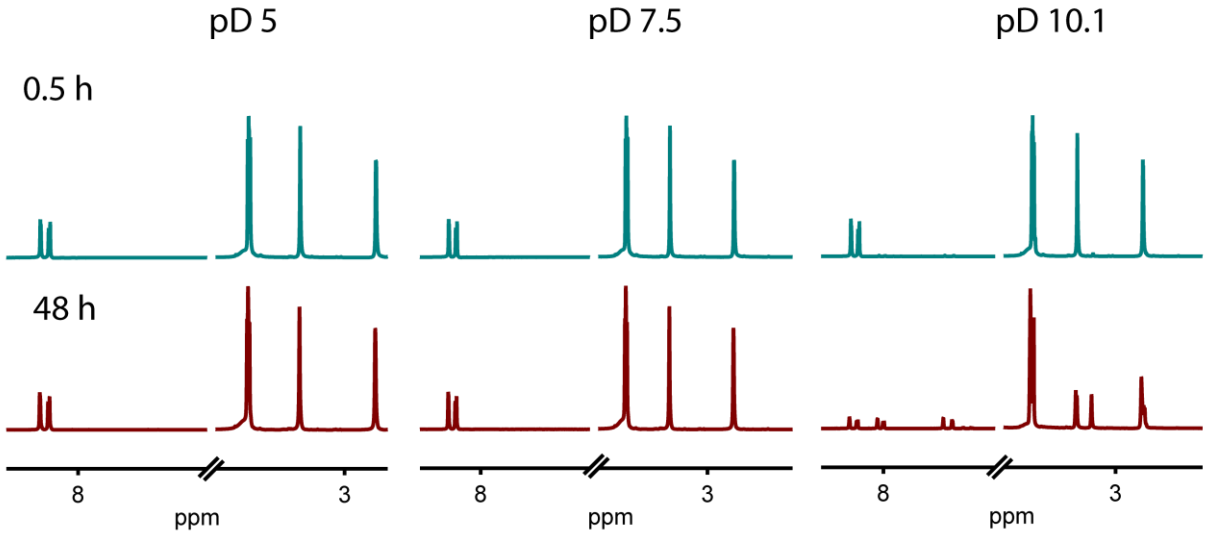

Figure 2.13. ^{1}H NMR degradation kinetics studies of diester diamide **8** in deuterated buffers.

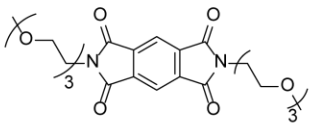

Bisimide **6**

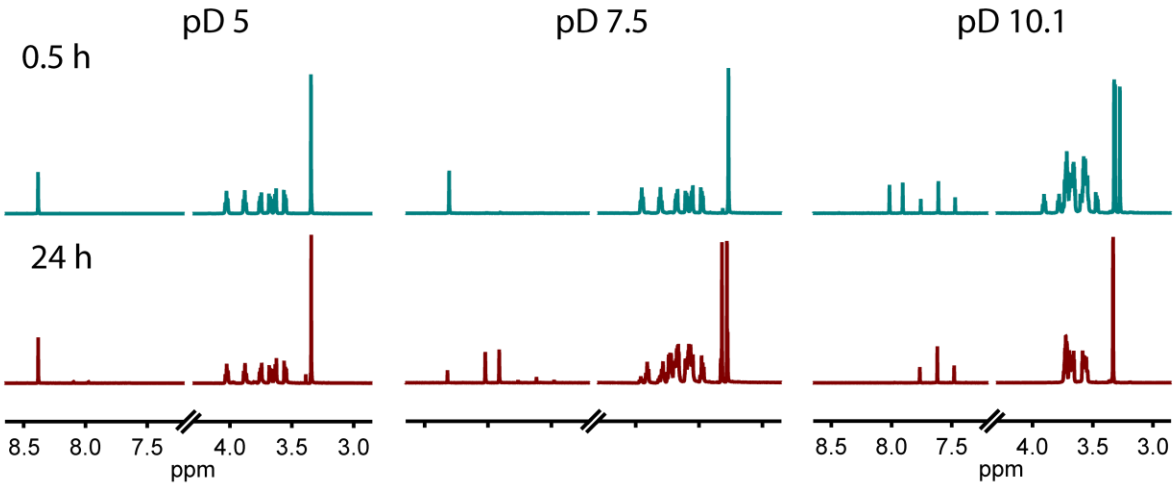

Figure 2.14. ^{1}H NMR degradation kinetics studies of bisimide **6** in deuterated buffers.

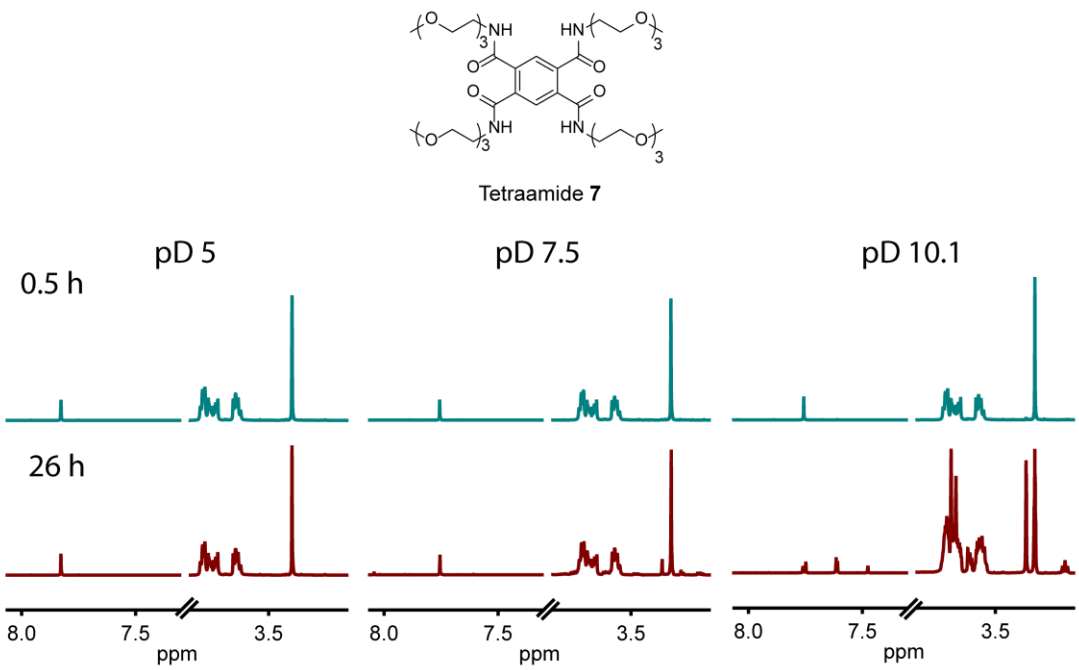

Figure 2.15. ^{1}H NMR degradation kinetics studies of tetraamide **7** in deuterated buffers in D_2O.

Additional evidence for the stability of the polymer capsules at pH 5 can be gleaned from the degrees of swelling in capsules at different pH values. Microcapsules were sprinkled on a thin film of polyurethane adhesive and cured for 24 h. The hardened adhesive patches with surface-lodged microcapsules were incubated in pH buffers and imaged under an optical microscope to determine the effect of pH on their diameters (**Figure 2.16**). The capsule diameter swelling ratios were calculated by dividing the average diameter measured in buffer by the average diameter of the dry capsules (see **Table 2.1**). At pH 5, a constant swelling ratio of 1.19 was observed at 1 and 4 days, whereas at pH 7.3, the swelling ratio increased slightly from 1.11 at 1 day to 1.13 at 4 days. The largest change in swelling ratio occurred at pH 10.3, starting at 1.31 at 1 day and reaching 1.7 at 4 days. The differences in swelling ratios could be attributed to increased hydrolytic cleavage of polymer chains at higher pH that decreased cross-linking and allowed the capsules to expand with increased solvent intake. Consistent with this notion, the trend in

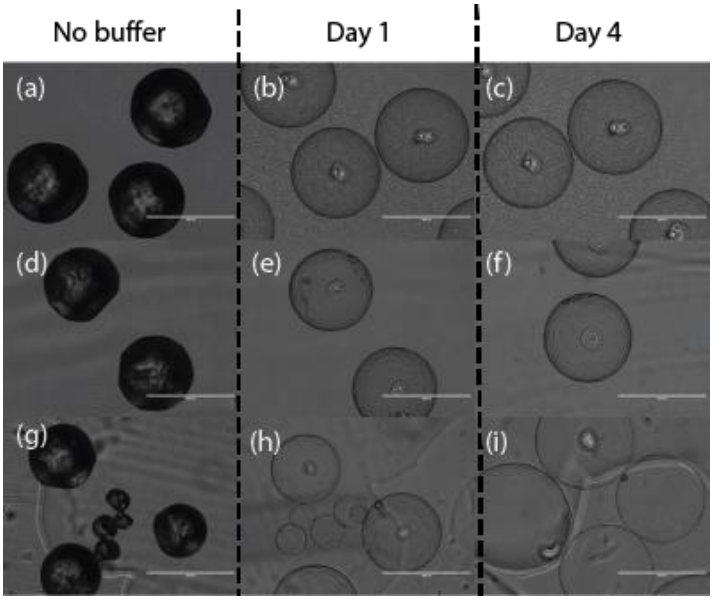

Figure 2.16. Optical micrographs of capsules: a), d), & g) before immersion in pH buffers; b-c) pH 5, e-f) pH 7.3, and h-i) pH 10.3. The scale bar is 400 μm.

Table 2.1. Swelling ratios of 1:1 triazine:DETA capsules in different buffers over time

pH	Day 1	Day 4
5	1.19 ± 0.04	1.19 ± 0.04
7.3	1.11 ± 0.01	1.13 ± 0.01
10.3	1.31 ± 0.09	1.7 ± 0.9*

* Most capsules detached from glue; ratio calculated by averaging 41 capsules on surface of glue from Day 4 and comparing to average of 21 capsules from Day 0. Uncertainty values reflected standard deviations of at least diameter measurements.

swelling ratios correlated with the relative stabilities observed in small-molecule degradation studies previously discussed. It is interesting to note that the constant swelling at pH 5 suggested the capsules responded to the pH 5 aqueous buffer in a consistent way, which fits the behavior predicted for a constant overall degree of protonation at a constant pH for a fixed amount of residual amine groups

A more direct test of the residual amine hypothesis would utilize zeta-potential measurements to assess the surface charge behavior of the microcapsules, which for a cationic polymer should

be more positive compared to control that has a lower amount of amines. However, attempts to analyze zeta potentials of the pulverized microcapsules shell polymer yielded inconsistent results, most likely because powders were difficult to disperse as an aqueous suspension that is necessary to acquire accurate zeta potential measurements. With the assistance from the Rienstra group, we turned to solid state NMR to identify and quantify the relevant functional groups within the shell polymer so that the charge states could be estimated. While functional groups differentiation proved to be challenging because of the similarity of functional groups as well as the significant peak broadening and overlap that are typical of crosslinked polymers, we identified from **Figure 2.17** a signal at a 53 ppm that likely represented the carbon peak of the methylene carbon alpha to the primary amine in DETA. The same methylene carbon is known to shift upfield to ca. 48 ppm upon conversion of the adjacent primary amine to an aromatic amide. Because all other amine or amide species in the polymer shell are expected to show methylene carbons peaks at less than 50 ppm, the presence of the 53 ppm peak in the solid state ^{13}C spectrum could be attributed to the presence of unreacted primary amine from the DETA monomer.

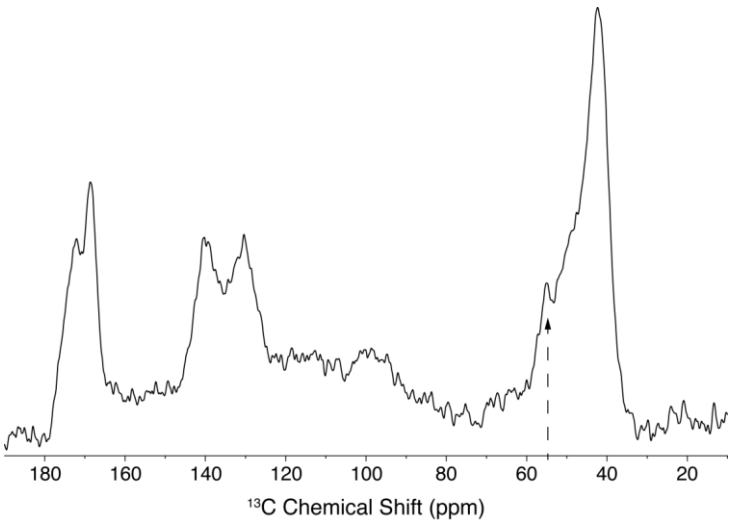

Figure 2.17. Solid state ^{13}C NMR of microcapsule polymer. The arrow points to a peak at ~ 55 ppm, which is consistent with the presence of unreacted DETA.

2.7 Solvent-triggered burst release

While the biphasic method adopted from literature successfully demonstrated pH-triggered release from the oil-core PDDC capsules, we also examined the release behavior under a single phase polar environment in an attempt to better elucidate the release behavior under a simpler triggering condition. Preliminary testing with 35 volume percent aqueous buffers in acetonitrile revealed that the microcapsules underwent rapid release with little dependence on the pH (**Figure 2.18**) suggesting that the main release mechanism under a polar organic solvent environment might not be pH-controlled.

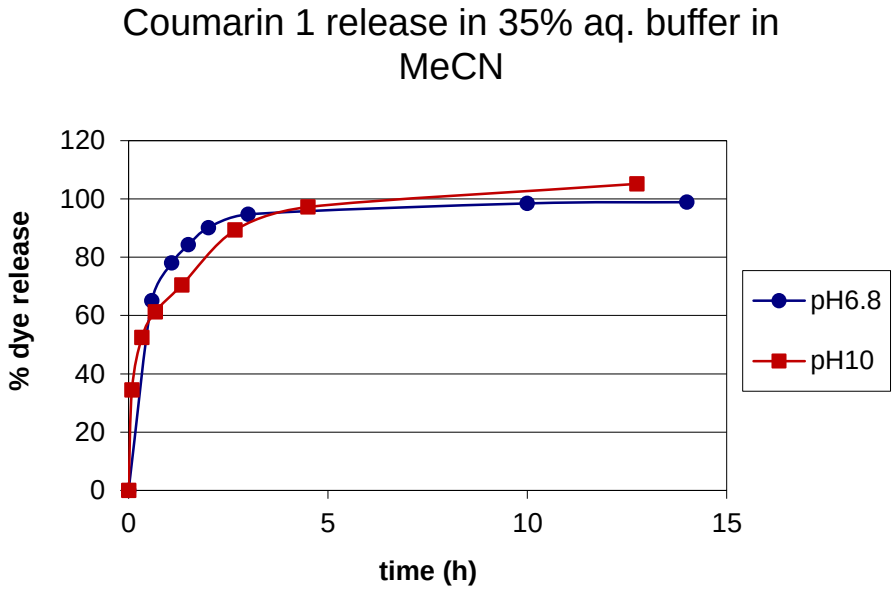

Figure 2.18. Microcapsules incubated in 35% aqueous buffers in acetonitrile at neutral and basic pH showed no significant difference in the rate of coumarin 1 release.

A plausible explanation is that small, highly polar organic (or mixture of organic/aqueous) solvent molecules better solvate and penetrate the highly crosslinked, polar microcapsule shells, thus allowing rapid permeation and leakage of core material. To test this hypothesis, the microcapsules were incubated in various alcoholic solvents of various sizes and polarities:

methanol, ethanol, 1-propanol, 2-propanol, and *tert*-butanol. Preliminary visual examination of the microcapsules (**Figure 2.19**) over the course of 24 h revealed that the majority of the microcapsules in methanol underwent rapid morphological changes to smoother spheres, followed by ruptures within 1 h. In ethanol, signs of core solvent loss (as indicated by a change to a lighter color within the microcapsules) were observed after several hours of incubation. All other higher alcohol solvents did not show visible changes to the incubated microcapsules in the same 24 h time period.

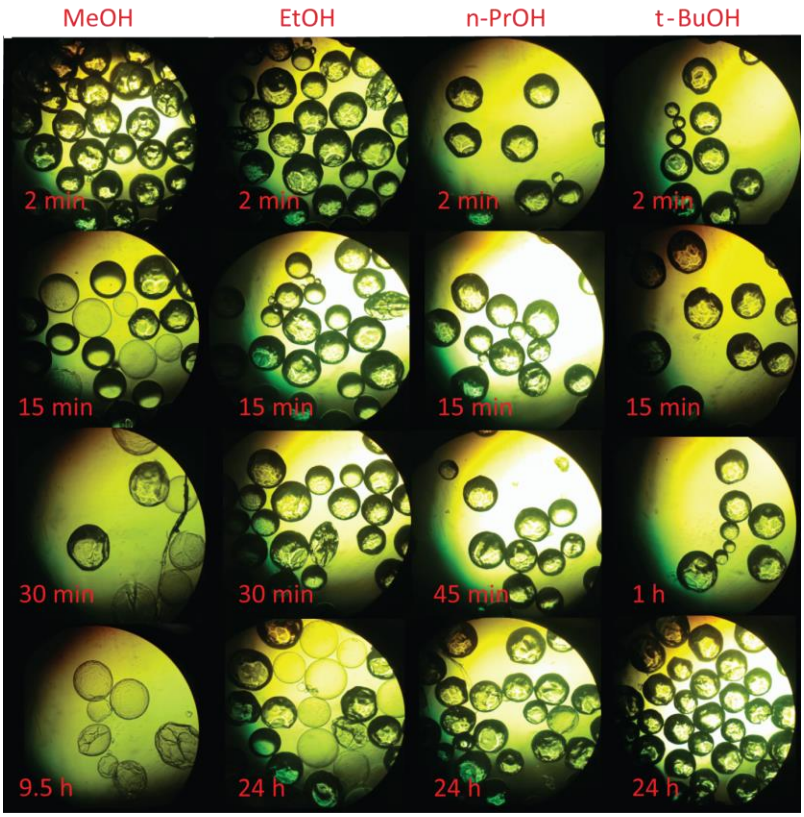

Figure 2.19. Time lapse images of microcapsules incubated in various alcoholic solvents.

The methanol experiment was reproduced under a video camera to capture the immediate swelling and bursting of the majority of the incubated microcapsules within 10 min of exposure to methanol. The observed phenomenon of burst release could be explained by selective

permeability of the shell to methanol and toluene that resulted in a rapid influx of methanol into the microcapsules and fast buildup of internal pressure that ruptured the shell.

However, it should be noted that this behavior did not occur in all microcapsules, which led to incomplete burst release. It is reasonable to attribute the difference in burst release rates to the polydisperse nature of microcapsules produced under mechanical agitation, which are a distribution of sizes and shell thicknesses that likely have different permeabilities and mechanical resistance to burst. The release behavior in ethanol appeared to be more subtle and only a small fraction of capsules showed signs of cracking, which could be a result of a slower diffusion into the microcapsules that led to a slower internal pressure buildup and only a small fraction of capsules had internal pressure that exceeded the burst threshold during the period of the experiment. The stability in higher alcohols suggested the possibility of tuning microcapsules triggered release by choice of added external solvents. The observed burst release behavior is an interesting area of investigation that could benefit from a highly controlled fabrication method of the microcapsules such as with flow-focusing microfluidics.

2.8 Conclusion and future outlook

In summary, we have developed a polyamide microcapsule using interfacial polymerization of a diester diacid chloride with DETA and a triazine trisamine to impart high loading capacity and dual acid/base-responsive properties. The preparation is sufficiently simple that it should be suitable to a larger-scale production level. To adjust the release profile, shell permeability was varied by altering the amine monomer feed ratio, demonstrating a simple tuning mechanism. The ability to retain a volatile core over a long period in a dry or hydrophobic state and to achieve different rates of small-molecule release over days when exposed to different pH suggests that this versatile pH-responsive microcapsule might be useful for applications such as fragrance

release on moist skin surfaces, alkaline laundry process, or delivery of pest control agents in agricultural settings. The use of the single encapsulation/release system for multiple environments is a key advantage of the chemistry described herein.

Finally, other experimentally observed behaviors such as the solvent-dependent bursting phenomenon of the PDDC polyamide microcapsules also invite further investigation into the detailed mechanism(s) of transport across the polymer barrier. Such an understanding would aid in the development of potential new applications such as in solvent-triggered burst release, high performance filtration, or oil separation and recovery from aqueous sources. We expect the use of flow-focusing microfluidics to fabricate microcapsules with narrow size dispersity and shell thickness will allow better controlled experiments to assess the capsule's materials properties and mechanisms of cargo release. Furthermore, encapsulation of actives with different molecular sizes and polarities will also elucidate the selective permeability of the microcapsules shell.

2.9 Experimental section

General Methods

All solvents and reagents were used as received unless otherwise noted. Anhydrous solvents were obtained from a MBraun SPS-800 Solvent Purification System. Common solvent and reagent names are abbreviated as followed: dichloromethane (DCM), diethyl ether (Et_2O), *N*,*N*-diisopropylethylamine (DIPEA), dimethylformamide (DMF), ethyl acetate (EtOAc), ethanol (EtOH), tetrahydrofuran (THF), trifluoroacetic acid (TFA), and methanol (MeOH). Reaction temperatures reported were the temperatures of the heating or cooling medium. Column chromatography was performed using flash silica gel (40-63 μm, 230-400 mesh). Unless otherwise noted, ^{1}H NMR and ^{13}C NMR spectra were obtained on a 500 MHz Varian instrument (U500 or VXR500) at the VOICE NMR laboratory at the University of Illinois at Urbana-

Champaign. Chemical shifts are reported in parts per million (ppm) and coupling constants in Hertz (Hz). NMR spectra obtained in $CDCl_3$ were referenced to 7.26 ppm for ^1H and 77.16 ppm for ^{13}C; methanol-d_4 was referenced to 3.31 ppm for ^1H and 49.00 ppm for ^{13}C; DMSO-d_6 was referenced to 2.50 ppm for ^1H and 39.52 ppm for ^{13}C. ESI mass spectra were obtained at the Mass Spectrometry Center at the University of Illinois at Urbana-Champaign. UV-visible spectroscopic measurements were performed on a Shimadzu UV-2501PC instrument using a 1.5 mL quartz cuvette with a path length of 1 cm. FT-IR was obtained on a *Nicolet Nexus 670 ATR instrument*. Scanning electron microscopy was performed on an FEI^{TM} Quanta FEG 450 environmental scanning electron microscope at the Imaging Technology Group of the Beckman Institute at the University of Illinois at Urbana-Champaign. Digital micrographs were obtained on an AMG EVOS *fl* digital inverted microscope from Prof. Martin Burke's lab. Nanomechanical measurements were performed on a Hysitron TI 950 TriboIndenter at the Frederick Seitz Materials Research Laboratory at the University of Illinois at Urbana-Champaign.

Synthetic Procedures

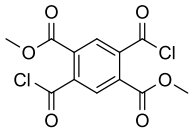

PDDC, **1**. To a 100 mL round bottom flask under N_2 was added 2.7 g (9.6 mmol) of 2,5-dicarbomethoxy terephthalic acid[29] (pyromellitic diester diacid) and 20 mL of anhydrous DCM. The suspension was stirred and 1.9 mL (22 mmol) of oxalyl chloride and 0.2 mL (3 mmol) of anhydrous DMF were added. Vigorous bubbling was observed for first 3 min and gradually slowed down; the solution became clear in 8 h. The solvent was removed *in vacuo*. The solid residue was dissolved in 50 mL anhydrous DCM and concentrated *in vacuo* to afford 3.0 g (98%)

of **1** as a white powder. ^{1}H NMR (DMSO-d_6): δ 8.01 (s, 2H), 3.84 (s, 6H). ^{13}C NMR (DMSO-d_6): δ 166.4, 166.3, 134.3, 134.2, 128.8, 52.9.

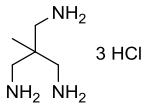

Tirs(aminomethyl)ethane trihydrochloride **2**. The trihydrochloride salt of TAME was synthesized from catalytic reduction of a literature known tribenzylamine trihydrochloride.[30] To a 100 mL 3-neck roundbottom flask, a filtered, 5 mL methanol solution of 0.5 g (1 mmol) tribenzylamine trihydrochloride precursor was added and diluted with ca. 40 mL methanol. A condenser was fitted and the stirring benzylamine solution was degassed by gentle evacuation until bubbling and nitrogen backfilling. The degas procedure was repeated two times. The stirring solution was quickly added 0.1 g 10 wt% Pd on carbon powder and 0.94 g (15 mmol) ammonium formate crystals. The degas procedure was repeated four times. The solution was heated to reflux for 5.5 h, cooled to r.t., and vacuum filtered through a bed of celite, which was rinsed with additional methanol to keep the bed of celite with filtered Pd/C powder moist. The filtrate was concentrated invacuo to yield a white solid that was suspended in hot DI water and passed through a 0.45 µm syringe filter to removed insoluble particulates. The aqueous solution was lyophilized over 2 days to afford 0.17 g (75%) of a white solid. ^{1}H NMR (CD_3OD-D_2O): δ 3.13 (s, 6H), 1.21 (s, 3H). ^{13}C NMR (CD_3OD-D_2O): δ 45.5, 36.0, 18.1. ESI-HRMS: calculated 118.1344, found 118.1348, $C_5H_{16}N_3$ $[M+H]^+$

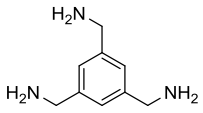

1,3,5-tris(aminomethyl)benzene **3**. The full synthesis of 1,3,5-tris(aminomethyl)benzene started from a one-pot reduction-bromination[31] of trimethyl 1,3,5-benzenetricarboxylate to afford 1,3,5-

tris(bromomethyl)benzene in 85% yield, which was followed by an azidation reaction[32] to form 1,3,5-tris(azidomethyl)benzene in 48% yield. The final catalytic hydrogeation[33] of the triazide yielded 0.69 g (92%) of a yellow solid product, whose NMR characterization was consistent with literature.

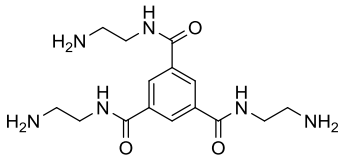

Tris(2-aminoethyl)-1,3,5-benzenetricarboxylamide **4**. The aromatic triamide was synthesized according to literature[34], yielding 0.53 g (75%) of a white solid. ^{1}H NMR (DMSO-d_6): δ 8.49 (s br, 3H), 8.21 (s, 3H), 3.09 (d, J = 6, 6H), 2.50 (t, J = 6, 6H), 1.99 (s br, 6H). ^{13}C NMR (DMSO-d_6): δ 165.7, 135.1, 128.5, 43.2, 80.0, 40.5, 41.3. ESI-HRMS: calculated 337.1988, found 337.1985, $C_{15}H_{25}N_6O_3$ $[M+H]^+$

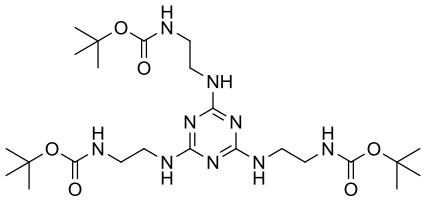

2,4,6-Tris[2-(*N*-*tert*-butoxycarbonyl)ethylamino)]-1,3,5-triazine was synthesized according to literature procedure.[35] To 400 mL of toluene was added 7.0 g of cyanuric chloride (39 mmol) and stirred under N_2. A solution of 34 g of *N*-Boc-ethylenediamine (212 mmol) and 40 mL of *N*,*N*-diisopropylethylamine in 400 mL of toluene was added. The resulting white suspension was heated to reflux for 12 h, cooled to room temperature, and vacuum filtered. The filtered yellowish white solid was dissolved using 300 mL of boiling $CHCl_3$ and 50 mL of DI H_2O. After cooling to room temperature, the biphasic solution was separated and the cloudy organic layer was washed with DI H_2O (300 mL x 3) and brine (300 mL). The clear organic layer was dried

over Na_2SO_4 and concentrated *in vacuo* to a foamy solid. Recrystallization from 500 mL of boiling toluene and afforded 19.4 g (84%) white solid powder. ^{1}H NMR (CD_3OD): δ 3.38 (m, br, 6H), 3.22 (s, br, 6H), 1.42 (s, 27H). ^{13}C NMR (CD_3OD): δ 167.3, 158.4, 80.0, 40.5, 40.4, 28.8. mp: 169.5-170.8 ℃. ESI-HRMS: 556.3571 calculated, 556.3569 found, $C_{24}H_{46}N_9O_6$ $[M+H]^+$.

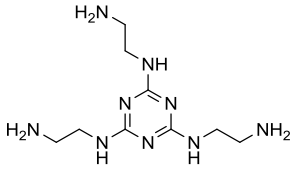

Triazine crosslinker **5**. To a stirred suspension of 12 g of 2,4,6-tris[2-(*N*-*tert*-butoxycarbonyl) ethylamino)]-1,3,5-triazine (26 mmol) in 120 mL of DCM was slowly added 60 mL (784 mmol) of TFA. The suspension turned into a clear, light yellow solution with vigorous bubbling that lasted approximately 10 min. The solution was stirred for 2.5 h, concentrated *in vacuo* to give a clear yellow viscous oil. Dissolution and evaporation with 100 mL of MeOH four times afforded a foamy solid that was dissolved in 10 mL of DI H_2O and 150 mL of 8 M aqueous NaOH to give a cloudy suspension. The aqueous suspension was extracted five times with 200 mL of $CHCl_3$ until the aqueous layer turned mostly clear. The combined organic layers was dried over Na_2SO_4 and concentrated *in vacuo* to afford 3.5 g (63%) of **2** as a clear yellow viscous oil. ^{1}H NMR (CD_3OD): δ 2.85 (t, J = 6, 6H), 3.41 (s, br, 6H). ^{13}C NMR (CD_3OD): δ 165.9, 42.7, 40.5. ESI-HRMS: calculated 256.1988, found 256.1988, $C_9H_{22}N_9$ $[M+H]^+$.

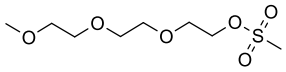

Methane sulfonyl tri(ethylene glycol) monomethyl ether was prepared according to literature procedure.[36] Additional purification by column chromatography using a gradient elution from 90% (v/v) EtOAc in hexanes to 100% EtOAc afforded the pure product in 66% yield. ^{1}H and ^{13}C NMR spectra were consistent with literature. ESI-MS: 265.1 $[M+Na]^+$.

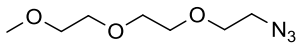

To a 500 mL round bottom flask was added 22.5 g of methane sulfonyl tri(ethylene glycol) monomethyl ether (93 mmol), 6.6 g of sodium azide (102 mmol) and 150 mL of DMF under N_2. The solution was heated at 60 ^oC for 24 h and the mixture solidified. With continued heating, 50 mL of DMF was added to dissolve the solid. The solution was heated an additional 6 h, cooled to room temperature, and poured into 400 mL of DI H_2O. The aqueous solution was extracted three times with 200 mL of Et_2O. The combined organic layer was dried over Na_2SO_4 and concentrated *in vacuo* to afford 8.8 g (50%) of yellow oil. ^1H NMR ($CDCl_3$): δ 3.69-3.63 (m, 8H) 3.56-3.53 (m, 2H), 3.40-3.36 (m, 5H). ^{13}C NMR ($CDCl_3$): δ 72.0, 70.83, 70.80, 70.7, 70.2, 59.2, 50.8. ESI-MS: 212.1 $[M+Na]^+$.

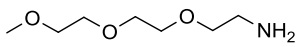

To a solution of 8.8 g 1-azido-2-(2-(2-methoxyethoxy)ethoxy)ethane (47 mmol) in 55 mL of THF was added 13.3 g of triphenyl phosphine (51 mmol) and stirred for 12 h at room temperature under N_2. To the solution was added 80 mL of DI H_2O and the mixture stirred for 12 h. The volume of solution was reduced by 50 mL *in vacuo* and the precipitate was filtered off by vacuum filtration. The collected solid was washed with DI H_2O, and the filtrates were combined to give a total volume of approx. 120 mL. The combined filtrate was washed with DCM (2 x 50 mL) and toluene (2 x 50 mL). The clear aqueous layer was concentrated *in vacuo* to afford 6 g (79%) of a yellow oil. ^1H NMR ($CDCl_3$): δ 3.62-3.56 (m, 6 H), 3.52-3.48 (m, 2H), 3.45 (t, J = 5, 2H), 3.32 (s, 3H), 2.80 (t, J = 5, 2H), 1.38 (s br, 2H). ^{13}C NMR ($CDCl_3$): δ 73.5, 72.0, 70.63, 70.57, 70.3, 59.1, 41.8. ESI-MS: 164.1 $[M+H]^+$.

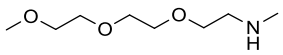

Methane sulfonyl tri(ethylene glycol) monomethyl ether (0.50 g, 1.9 mmol) and 5.0 mL of 33 wt% methylamine in EtOH were added under N_2 and stirred overnight. The solution was concentrated *in vacuo* and purified by silica column chromatography in 1:9:90 (v/v/v) NH_4OH/MeOH/DCM to afford 0.22 g of a yellow oil. NMR analysis suggested a mostly pure product was obtained, which was used directly in the synthesis of **6** without further removal of residual methanol and dichloromethane solvents. ^{1}H NMR ($CDCl_3$): δ 3.63-3.58 (m, 6H), 3.56 (t, J = 5, 2H), 3.54-3.50 (m, 2H), 3.35 (s, 3H), 2.73 (t, J = 5, 2H), 2.40 (s, 3H). ^{13}C NMR ($CDCl_3$): δ 71.9, 70.6, 70.5, 70.3, 70.0, 59.1, 51.1, 36.1. ESI-MS: 178.09 $[M+H]^+$.

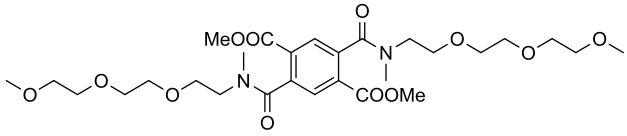

Diester diamide **6**. To a 15 mL round bottom flask under N_2 was added 0.184 g diacid chloride **1** (5.95 mmol) and the solids were stirred in 1 mL anhydrous DCM until dissolved. A mixture of 0.2 g 2-(2-(2-methoxyethoxy)ethoxy) ethyl-*N*-methylamine (1 mmol) and 0.2 mL DIPEA (1 mmol) in 1 mL anhydrous DCM was syringed dropwise into solution of **1**. The solution was stirred overnight and concentrated *in vacuo* to give a yellow waxy solid that was purified by silica column chromatography using a gradient elution from 5 to 10% (v/v) MeOH in DCM to afford 0.23 g (67%) of **6** as a clear, slightly yellow viscous oil. ^{1}H NMR ($CDCl_3$): δ 7.98-7.87 (m, 2 H), 3.91-3.84 (m, 6 H), 3.83-3.42 (m, 24 H), 3.34 (s, 6 H), 3.16 (s, 2 H), 2.85 (s, 4 H). ^{13}C NMR ($CDCl_3$): δ 169.85, 169.82, 169.66, 169.63, 164.91, 164.82, 139.49, 139.46, 139.27, 139.24, 131.2, 131.0, 130.9, 130.7, 130.2, 130.1, 129.4, 129.3, 72.2,72.1, 70.9, 70.8, 70.77, 70.75, 70.6, 69.4, 68.9, 68.8,59.3, 53.09, 53.07, 53.04, 53.01, 50.7, 47.4, 38.4, 33.4 (peaks doubled as a

result of conformational isomers). ESI-HRMS: calculated 601.2972, found 601.2971, $C_{28}H_{45}N_2O_{12}$ $[M+H]^+$.

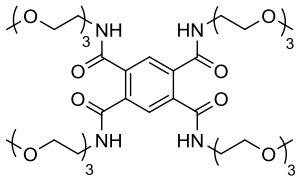

Tetraamide **5**. To a 15 mL round bottom flask was added 800 mg of 2-(2-(2-methoxyethoxy)ethoxy)-ethan-1-amine (4.9 mmol) and 0.25 mL DIPEA (1.4 mmol) under N_2. The mixture was added 51 mg diacid chloride **1** (0.16 mmol) and the suspension was stirred at room temperature under N_2. Addition of 1 mL of anhydrous THF completed the dissolution of suspended solids and the solution was stirred overnight. Evaporation of solvent *in vacuo* gave a yellow oil that was purified by silica column chromatography using a gradient elution from 5 to 10% (v/v) MeOH in DCM to afford 80 mg (60%) of **5** as a waxy solid. ^{1}H NMR ($CDCl_3$): δ 7.77 (s, 2H), 7.55 (s br, 4H), 3.70-3.56 (m, 40H), 3.49-3.44 (m, 8H), 3.27 (s, 12H). ^{13}C NMR ($CDCl_3$): δ 167.8, 136.5, 128.7, 71.9, 70.6, 70.5, 70.4, 69.6, 59.0, 40.2. ESI-HRMS: calculated 835.4552, found 835.4520, $C_{38}H_{67}N_4O_{16}$ $[M+H]^+$.

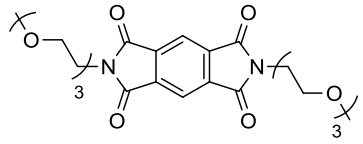

Bisimide **4**. To a 50 mL three-neck round bottom flask was added 0.25 g of diacid chloride **1** (0.78 mmol) and 2 mL of anhydrous dichloromethane. The suspension was stirred at room temperature until dissolved. The homogenous solution was cooled in a -78 ℃ dry ice-isopropanol bath and a solution of 0.28 g 2-(2-(2-methoxyethoxy)ethoxy)ethan-1-amine (2.7 mmol) and 0.3 mL DIPEA (1.7 mmol) was added dropwise. The resulting suspension turned

clear after 5 min, and was allowed to stir for 1 h. Solvent was removed *in vacuo* to give a yellow oil that was purified by silica column chromatography using a gradient elution from 50% to 80% (v/v) EtOAc in hexanes. The isolation of the first major spot on TLC afforded 0.17 g of a waxy white solid that was confirmed to be the bisimide **4** in a yield of 43%. ^{1}H NMR ($CDCl_3$): δ 8.25 (s, 2H), 3.95 (t, *J* = 5.5, 4H), 3.76 (t, *J* = 5.5, 4H), 3.67-3.62 (m, 4H), 3.61-3.55 (m, 8H), 3.50-3.46 (m, 4H), 3.33 (s, 6H). ^{13}C NMR ($CDCl_3$): δ 166.2, 137.3, 118.3, 72.0, 70.7, 70.67, 70.2, 67.8, 59.1, 38.0. ESI-HRMS: calculated 509.2135, found 509.2137 $C_{24}H_{33}N_2O_{10}$ $[M+H]^+$.

General Procedure for Preparation of PDDC and TC Microcapsules

A 0.090 M solution of diacid chloride (PDDC **1** or TC) and coumarin 1 dye (2 mg dye/mL) in toluene was added to 3 mL of aqueous polyvinyl alcohol (0.4 wt%, Mw 31,000-50,000, 87-89% hydrolyzed) in a 15 mL round bottom flask. The biphasic solution was emulsified with maximum magnetic stirring (1500 RPM) for 3 min on an IKA RCT basic magnetic stir plate until a uniformly cloudy suspension of emulsion droplets was formed. The stir rate was reduced to 900 RPM. A 1.5 mL aqueous solution of polyamines, prepared by mixing 1.5 M triazine **2** with the desired amount of DETA, was added dropwise. After the addition of the aqueous polyamines was complete, the suspension was further stirred for 30 sec. The suspension was cured for 60 min and diluted with 5 mL DI H_2O and vacuum filtered through Whatman Grade 1 filter paper. The collected microcapsules were rinsed with 100 mL DI H_2O, 100 mL acetone, and 20 mL Et_2O. The free flowing powder was allowed to air dry for at least 24 h.

Note: The amine – acyl chloride ratios were 65:1 and 44:1 respectively for the 1:1 and 3:1 triazine:DETA formulations. The large excess of amines ensures rapid shell formation by

enhanced diffusion of the amines into the hydrophobic droplet and serves to quickly neutralize the HCl generated from the polycondensation reaction.

General Procedure for Dye Release Experiments

Percent dye release was normalized against experimentally determined dye content in microcapsules (i.e., mg of dye per mg of capsules). The dye content was determined by shredding weighed microcapsules suspended in toluene by 5 min sonication in a sonicator bath (Fisher Scientific FS100; completion of capsule shredding was confirmed by examination with an optical microscope) and assaying the toluene layer with UV-vis.

With toluene: Approximately 15 mg of microcapsules was immersed in 20 mL toluene in a capped scintillation vial and placed on an orbital shaker at approx. 60 RPM. The supernatant was assayed with UV-vis periodically.

With pH buffers and toluene: Same as toluene control except the microcapsules were suspended between 10 mL of toluene and 5 mL of aqueous pH buffer. For microcapsules prepared with 20 mg/mL dye solution, 150 mL of toluene and 50 mL of aqueous pH buffer were used.

Solid state ^{13}C NMR

The spectrum in Figure 16 was obtained on a 600 MHz Varian InfinityPlus with a 3.2 mm HCN triple resonance Balun probe. The total acquisition time was 28.8 h and the magic-angle spinning rate was 11.111 kHz.

2.10 References

(1) Binauld, S.; Stenzel, M. H. *Chemical Communications* **2013**, *49*, 2082.

(2) Esser-Kahn, A. P.; Odom, S. A.; Sottos, N. R.; White, S. R.; Moore, J. S. *Macromolecules* **2011**, *44*, 5539.

(3) Wang, H.-C.; Zhang, Y.; Possanza, C. M.; Zimmerman, S. C.; Cheng, J.; Moore, J. S.; Harris, K.; Katz, J. S. *ACS Appl. Mater. Interfaces* **2015**, *7*, 6369.

(4) Okahata, Y.; Noguchi, H.; Seki, T. *Macromolecules* **1987**, *20*, 15.

(5) Sukhorukov, G. B.; Antipov, A. A.; Voigt, A.; Donath, E.; Möhwald, H. *Macromol. Rapid Commun.* **2001**, *22*, 44.

(6) De Geest, B. G.; Van Camp, W.; Du Prez, F. E.; De Smedt, S. C.; Demeester, J.; Hennink, W. E. *Macromol. Rapid Commun.* **2008**, *29*, 1111.

(7) Esser-Kahn, A. P.; Sottos, N. R.; White, S. R.; Moore, J. S. *J. Am. Chem. Soc.* **2010**, *132*, 10266.

(8) Broaders, K. E.; Pastine, S. J.; Grandhe, S.; Frechet, J. M. J. *Chem. Commun.* **2011**, *47*, 665.

(9) Abbaspourrad, A.; Datta, S. S.; Weitz, D. A. *Langmuir* **2013**, *29*, 12697.

(10) Ejima, H.; Richardson, J. J.; Liang, K.; Best, J. P.; van Koeverden, M. P.; Such, G. K.; Cui, J.; Caruso, F. *Science* **2013**, *341*, 154.

(11) Grolman, J. M.; Inci, B.; Moore, J. S. *ACS Macro Lett.* **2015**, *4*, 441.

(12) Baker, J. P.; Stephens, D. R.; Blanch, H. W.; Prausnitz, J. M. *Macromolecules* **1992**, *25*, 1955.

(13) Kashiwabara, M.; Fujimoto, K.; Kawaguchi, H. *Colloid Polym. Sci.*, *273*, 339.

(14) Das, M.; Kumacheva, E. *Colloid Polym. Sci.* **2006**, *284*, 1073.

(15) Georgiou, T. K.; Patrickios, C. S. *Biomacromolecules* **2008**, *9*, 574.

(16) Walter, H.; Harrats, C.; Müller-Buschbaum, P.; Jérôme, R.; Stamm, M. *Langmuir* **1999**, *15*, 1260.

(17) Kozlovskaya, V.; Sukhishvili, S. A. *Macromolecules* **2006**, *39*, 6191.

(18) Kudaibergenov, S. E.; Nuraje, N.; Khutoryanskiy, V. V. *Soft Matter*.**2012**, *8*, 9302.

(19) Ng, L.-T.; Ng, K.-S. *Radiat. Phys. Chem.* **2008**, *77*, 192.

(20) Barcellona, M. N.; Johnson, N.; Bernards, M. T. *Langmuir* **2015**, *31*, 13402.

(21) Andrade, B.; Song, Z.; Li, J.; Zimmerman, S. C.; Cheng, J.; Moore, J. S.; Harris, K.; Katz, J. S. *ACS Appl. Mater. Interfaces* **2015**, *7*, 6359.

(22) Fessi, H.; Briancon, S. p.; Puel, F. ß. *Microencapsulation* **2005**, 149.

(23) Morgan, P. W.; Kwolek, S. L. *J. Chem. Educ.* **1959**, *36*, 182.

(24) Mathiowitz, E.; Cohen, M. D. *J. Memb. Sci.* **1989**, *40*, 1.

(25) Wörl, R.; Köster, H. *Tetrahedron* **1999**, *55*, 2941.

(26) Mathiowitz, E.; Cohen, M. D. *J. Memb. Sci.* **1989**, *40*, 27.

(27) Janssen, L. J. J. M.; te Nijenhuis, K. *J. Memb. Sci.* **1992**, *65*, 59.

(28) Pastine, S. J.; Okawa, D.; Zettl, A.; Fréchet, J. M. J. *J. Am. Chem. Soc.* **2009**, *131*, 13586.

(29) Park,S.K.; Park,S.Y.; Lee,C.J. *Polymer* **2000**, *41*, 433.

(30) Qin, C.-J.; James, L.; Chartres, J. D.; Alcock, L. J.; Davis, K. J.; Willis, A. C.; Sargeson, A. M.; Bernhardt, P. V.; Ralph, S. F. *Inorg. Chem.* **2011**, *50*, 9131.

(31) Ilioudis, C. A.; Tocher, D. A.; Steed, J. W. *J. Am. Chem. Soc.* **2004**, *126*, 12395.

(32) Cecioni, S.; Argintaru, O.-A.; Docsa, T.; Gergely, P.; Praly, J.-P.; Vidal, S. *New J. Chem.* **2009**, *33*, 148.

(33) Granzhan, A.; Schouwey, C.; Riis-Johannessen, T.; Scopelliti, R.; Severin, K. *J. Am. Chem. Soc.* **2011**, *133*, 7106.

(34) Matsuura, K.; Murasato, K.; Kimizuka, N. *J. Am. Chem. Soc.* **2005**, *127*, 10148.

(35) Murasato, K.; Matsuura, K.; Kimizuka, N. *Biomacromolecules* **2008**, *9*, 913.

(36) McFarland, J. M.; Francis, M. B. *J. Am. Chem. Soc.* **2005**, *127*, 13490.

Chapter 3

Poly(hydroxyurethane-acetal)s: a new intramolecular mechanism for efficient polyacetal degradation

Collaboration and contribution statement:

The poly(hydroxyurethane-acetal) projects have been a collaboration among the dissertation author, Ephraim Morado, and Brittany Walker. The dissertation author and Ephraim Morado have contributed equally to the linear polymer project. Ephraim Morado has taken the lead on the microcapsules project with significant contribution to project design, precursor and capsules syntheses and characterization, while the dissertation author has contributed mainly to concept designs, troubleshooting, and materials characterizations. Brittany Walker has contributed to the syntheses of aromatic dicarbonate monomer and precursors for the linear polymer project as well as attempted direct poly(HU-acetal) synthesis using diisocyanate chemistry.

3.1 Introduction

Polyacetals are acetal containing polymers that undergo covalent bond breaking or exchange at the acetal centers in an acidic protic environment. In the presence of an activating acidic species (Broøsted or Lewis type) that coordinates to one of the acetal oxygen, the degradation of an acetal center is believed to occur through a rate determining formation of an oxocarbenium ion intermediate and concurrent ejection of the activated acetal oxygen species (**Scheme 3.1**).[1] In a protic environment, the reactive carbocation intermediate is quickly attacked by a surrounding protic species that gives up its proton to generate a new acetal (or, in the case of water acting as the nucleophilic species, a hemiacetal that can undergo another oxocarbenium ion formation to give up its second proton and generate a ketone or an aldehyde as a final product).

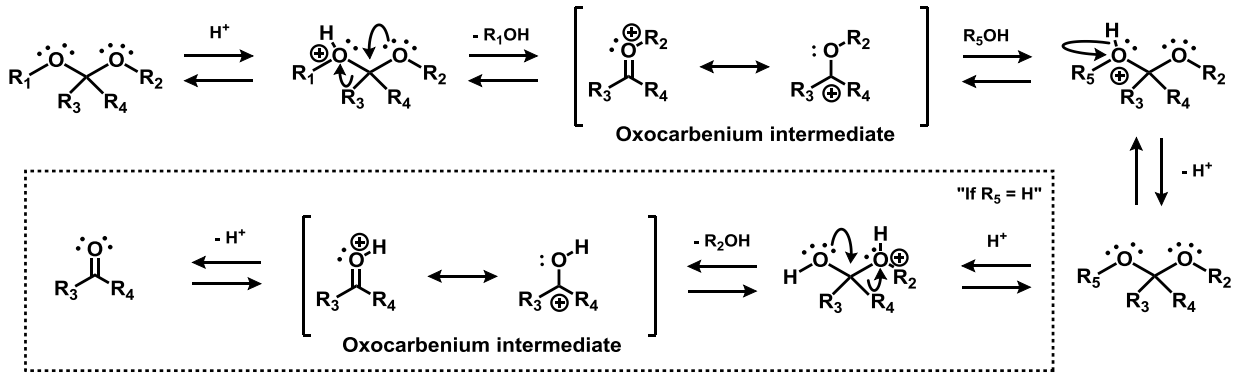

Scheme 3.1. Mechanism of acid-catalyzed acetal degradation, with H^+ indicating a generic acid that can either a Broøsted or Lewis type, and the dotted box indicating the case where R_5OH is a water molecule.

Because each step of the mechanism is a reversible process, the generation and destruction of acetals or polyacetals can be easily achieved by shifting the equilibrium to favor the desired species. The acid-catalyzed dynamic process of acetal formation and cleavage can be halted by scavenging the acid catalyst. For most acetals, a more basic environment increases the stability of the acetal moiety.

The tunable stability by modulation of the acid concentration makes polyacetals attractive for biomedical and drug delivery applications because in many diseased tissues, a lower than normal pH exists to allow a locally-triggered degradation of polyacetal-based medical devices or drug carriers.[2] The copious amount of body fluids in an acidic environment ensures continuous hydrolysis of acetal units in polyacetal materials. However, while thermodynamic factors are important to favor the desired equilibrium for polymer degradation, in real world applications kinetic considerations are also critical to achieve the targeted degradation rates. The reaction kinetics of acetal has been extensively investigated to suggest that factors such as the nature of adjacent substituents, steric effects, and hydrophobicity play a critical role in determining the reactivity of an acetal species.[3-5] For example, the formation of the oxocarbenium ion intermediate, which is rate limiting, can be favored or disfavored by an inductive effect from,

respectively, an electron donating or an electron-withdrawing group. Manipulation of the substituent effects to tune the reactivity of acetals is a popular strategy because of the abundance of structurally diverse, commercially or synthetically available aldehydes, ketones, and alcohols that permit a modular approach to designing acetal-based compounds and materials. In the case of hydrophobicity effect, a reasonable rationalization argues that a polar species such as an acid catalyst or a non-basic protic molecule is expected to experience greater difficulty penetrating and interact with a hydrophobic environment, and thus limiting access to the reactive acetal site.[5] It should be noted, however, few literature has investigated in detail an acid-catalyzed but anhydrous degradation condition for polyacetals, which is an important area of study given that many real world application environments have limited exposure to moisture, particularly in materials that are hydrophobic in nature.

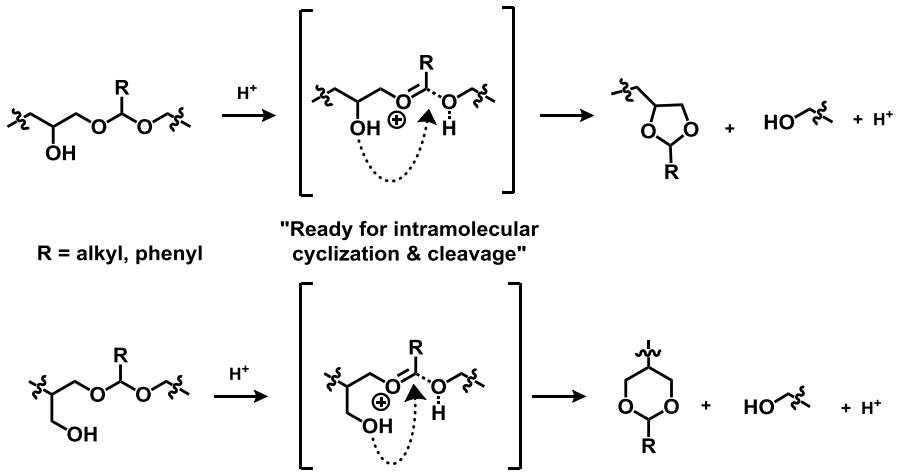

Scheme 3.2. Acid-catalyzed intramolecular cyclization to cleave an acyclic acetal and form a 5-membered (top) or 6-membered (bottom) cyclic acetal.

To attempt to address such deficiency in literature and achieve efficient acid-catalyzed depolymerization under a moisture-limited environment, we develop a novel acid-degradable poly(urethane-acetal) chemistry that utilizes intramolecular cyclization as the main mode of

acetal degradation. The key molecular design comes from a hydroxyl group that is four or five atoms away from an acyclic acetal carbon in a polyacetal (**Scheme 3.2**). In the presence of an acid catalyst, the hydroxyl group undergoes an intramolecular cyclization to form a cyclic acetal, which is expected to be less reactive than the starting acyclic acetal[6,7], and therefore effectively cleaves the polymer at the acetal repeat unit. One major advantage of the current design is the ability of the polyacetal to depolymerize without an exogenous protic reagent such as water, which is typically needed to efficiently degrade a polyacetal under an acidic condition. Depolymerization by intramolecular cyclization is a known strategy for cleaving urethane[8-10], ester[11-17], and carbonate[18,19] linkages. However, no polyacetal has been depolymerized using intramolecular acetal cyclization, to the best of our knowledge. Furthermore, the built-in hydroxyl groups in the polymer could lead to enhanced mechanical properties through increased hydrogen bonding between the polymer chains. Finally, the hydroxyl functionality could serve as an anchor for conjugation of releasable actives or other trigger-responsive moieties to introduce multimodal responsiveness to the designed polymeric materials.

3.2 Goals and approaches

Three different strategies (**Scheme 3.3**) aim to integrate the acid-degradable polyacetal design into a polyhydroxyurethane structure, each with its own set of predicted advantages. The first general design achieves isocyanate-free polyurethane formation by a step-wise polymerization of a diamine with a bis(cyclic carbonate) acetal to form poly(hydroxyurethane-acetal), or poly(HU-acetal). The opening of a cyclic carbonate moiety during the polymerization generates a primary or a secondary hydroxyl that is key to the proposed degradation mechanism. The second strategy utilizes a diamino acetal monomer, prepared from ring-opening of a bis(cyclic carbonate) acetal by two equivalents of a diamine, for polyamide formation with a polyacid chloride. Because the

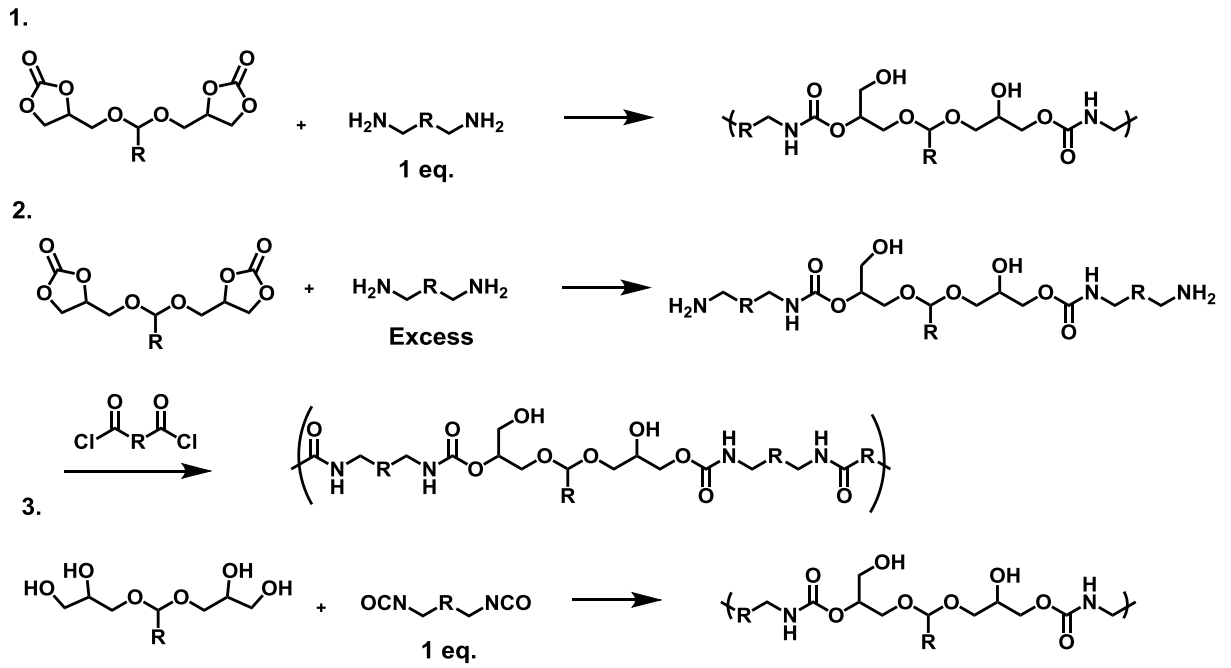

Scheme 3.3. The three proposed syntheses of poly(hydroxyurethane-acetal)s. The R group can be an alkyl or aromatic group that does not contain an acid scavenging functional group to prevent the sequestration of the acid catalyst.

diamino acetal monomer is expected to be water soluble, thin-shell microcapsules and thin films can be prepared by interfacial polymerization. Lastly, direct synthesis of poly(HU-acetal) from a diisocyanate and an acyclic acetal containing two sets of germinal diols (hereafter referred to as a tetrol acetal) can lead to linear or crosslinked polymers depending on reagent stoichiometry. The current work focuses on the development of the first two strategies.

3.3 Proof of concept with a small molecule analog

To assess the feasibility of acetal cleavage by intramolecular cyclization, a small molecule hydroxyurethane-acetal analog (**1**) of the acetal repeat unit was synthesized according to **Scheme 3.4** and subjected to acid and heat to determine its stability. The synthesis of **1** began with the preparation of diallyl acetal (**2**) in 64% yield from allyl alcohol and butyraldehyde in hexanes,

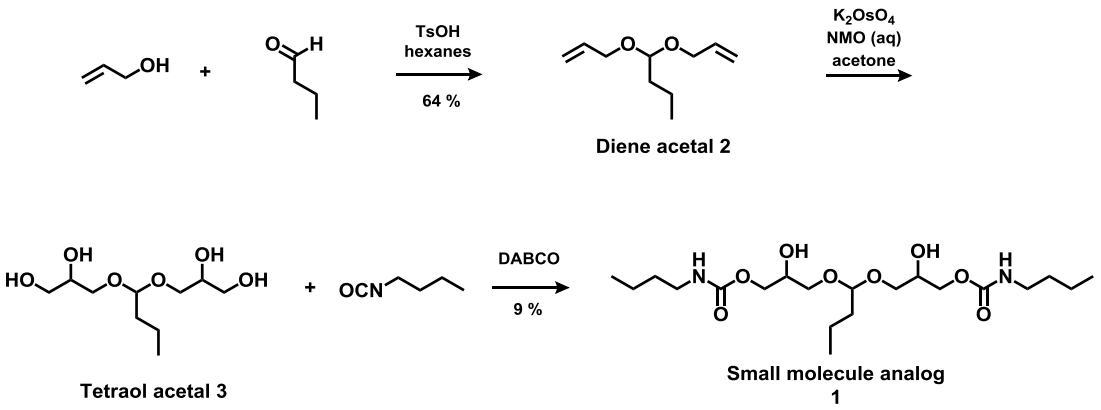

Scheme 3.4. Synthesis of small molecule analog **1**.

with *p*-toluenesulfonic acid (TsOH) as a strong acid catalyst and magnesium sulfate as the drying agent to sequester the water byproduct. Acetal **2** was dihydroxylated with catalytic amount of potassium osmate dihydrate in the presence of *N*-methylmorpholine oxide in acetone to afford mostly pure tetraol acetal (**3**) after silica column. The tetraol **3** was reacted, using DABCO as a base catalyst, with butyl isocyanate to give **1** with an un-optimized yield of 9%. The synthesis of **1** was confirmed by ^{1}H and homonuclear correlation spectroscopy (COSY) NMR experiments (**Figures 3.1a and b).**

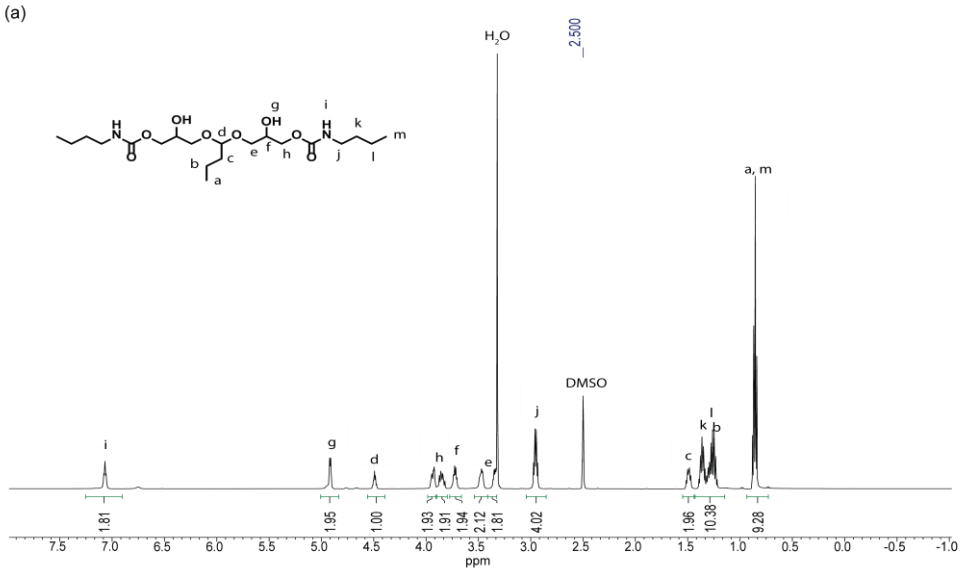

Figure 3.1a. ^{1}H NMR spectrum of analog **1** with assigned protons.

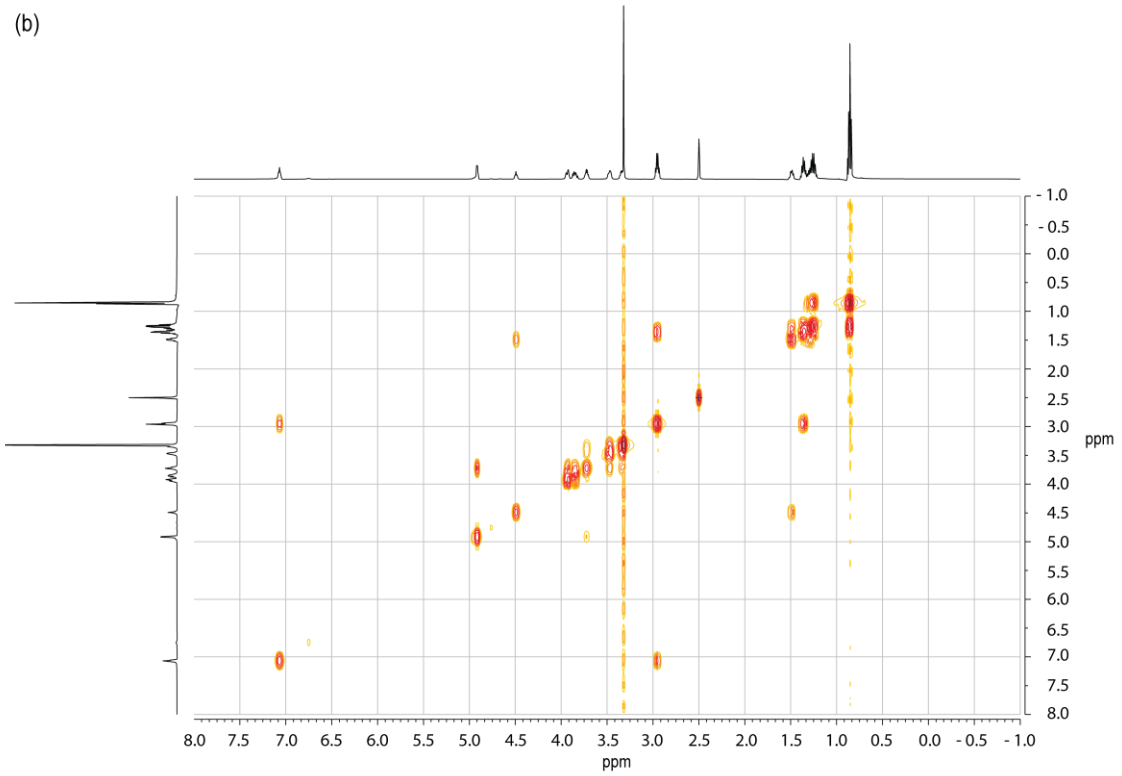

Figure 3.1b COSY spectrum of analog **1**.

The acid-catalyzed degradation of **1,** expected to follow the steps detailed in **Scheme 3.5**, was tracked by ^{1}H NMR. With 6 mol% dry TsOH dissolved in $CDCl_3$ that was pre-dried over 3Å molecular sieves, the degradation of **1** was completed within 2 h, with the formation of two new acetal peaks and no detectable aldehyde signal, suggesting the proposed degradation mechanism

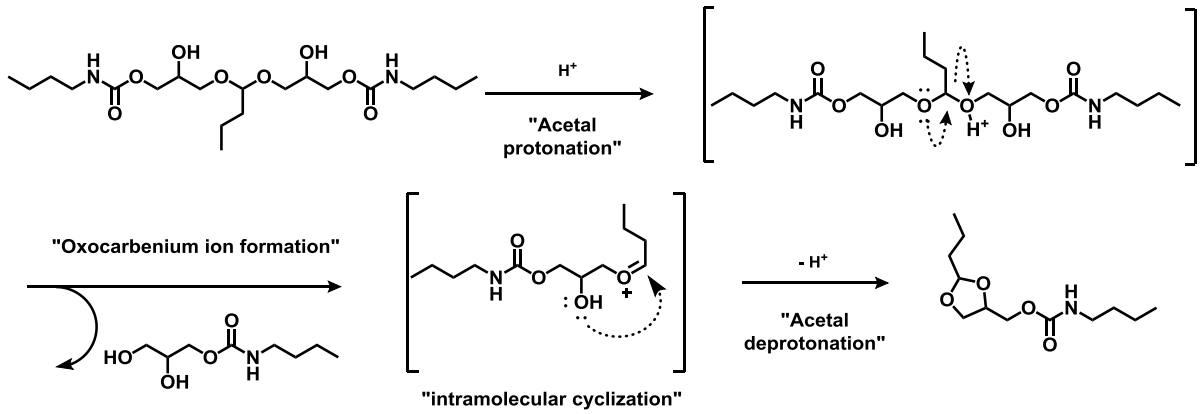

Scheme 3.5. Expected degradation of small molecule analog under acidic condition.

of intramolecular cyclization was operating. Analysis of triethylamine-quenched sample of degraded **1** using positive mode electrospray ionization mass spectrometry (ESI-MS) indicated the presence of the expected diol and cyclic acetal products (**Figure 3.2**).

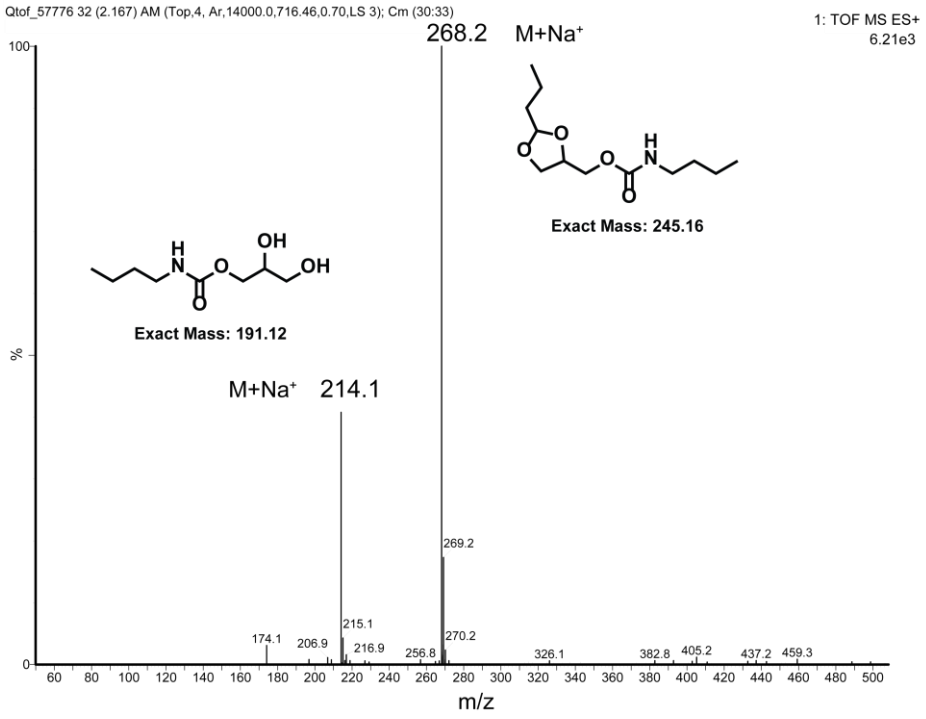

Figure 3.2. ESI+ mass spectrum from acid degradation experiment of **1** showing the presence of the expected diol and acetal products. (Note: line thicknesses and text sizes were enhanced using Adobe Illustrator for better visualization.)

A further NMR experiment (**Figure 3.3**) utilizing a lower TsOH concentration of 0.5 mol% in CD_3CN allowed for more careful tracking of the degradation kinetics. While a small amount (~7%) of aldehyde was detected, likely because of the residual water present in CD_3CN, the majority of degraded products exhibited new acetal peaks similar to those seen in the $CDCl_3$ experiment. As can be seen in **Figure 3.4**, the half-life of **1** was about 45 min. Thermal stability of **1** in a hydrophobic environment was confirmed by heating a toluene-d_8 solution of **1** at 95 ^oC for at least 10 h without any observable degradation (**Figure 3.5**).

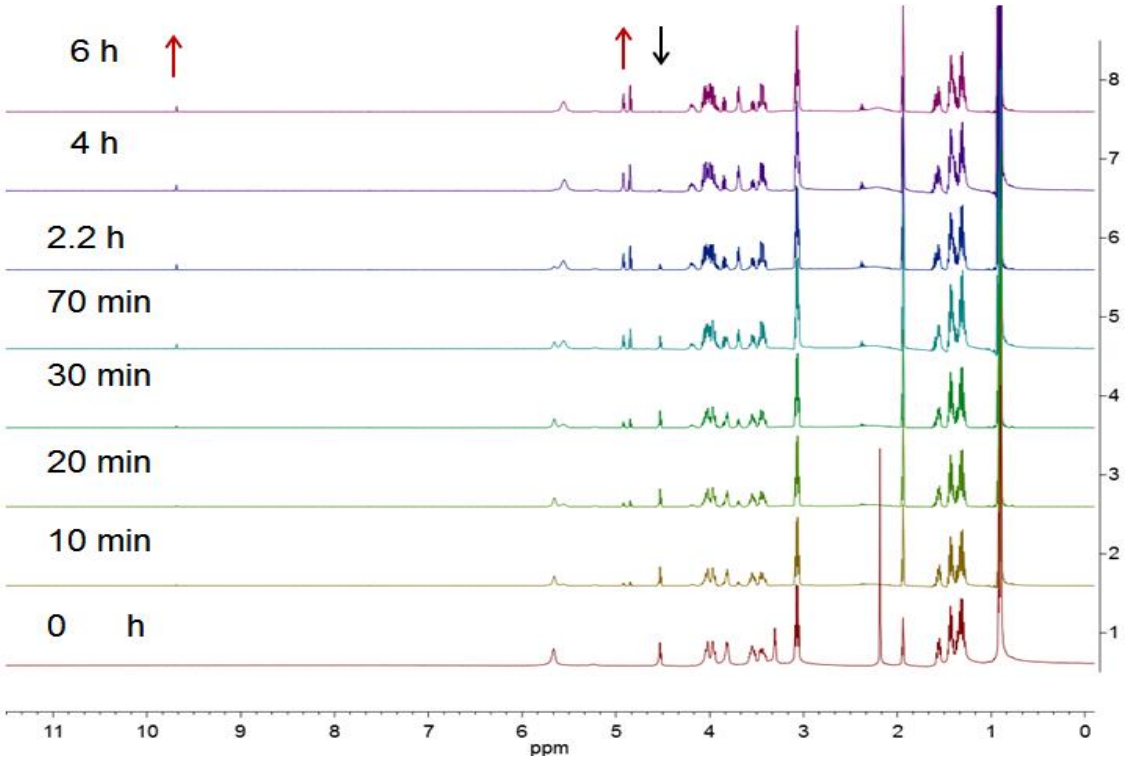

Figure 3.3. Stacked ^{1}H NMR spectra of analog **1** in 0.5 mol% TsOH in CD_3CN over 6 h.

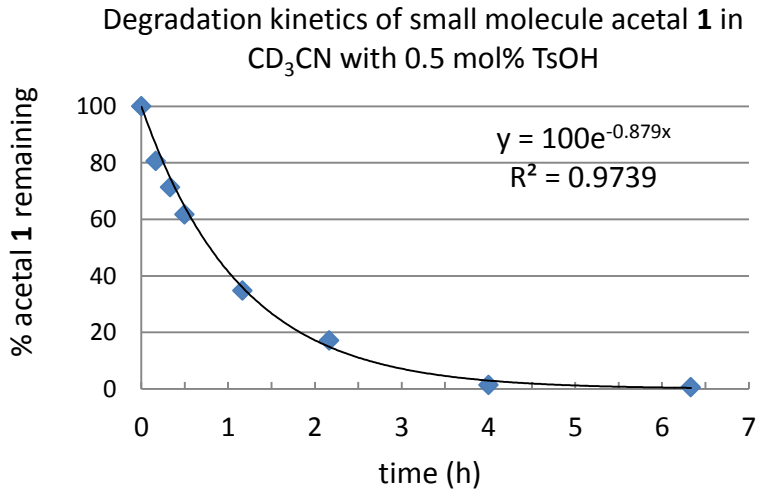

Figure 3.4. Degradation kinetics of small molecule analog **1** showing a first order decay profile.

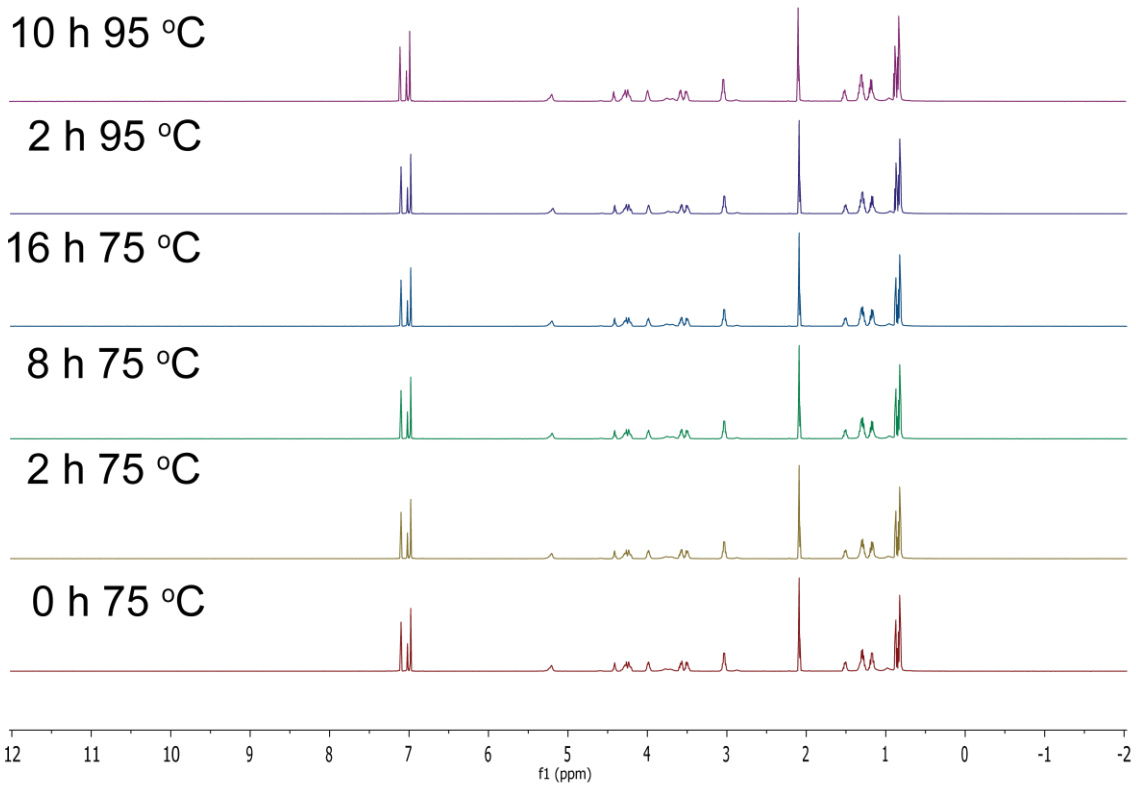

Figure 3.5. Thermal stability of analog **1** in toluene-d_8.

3.4 Linear poly(hydroxyurethane-acetal)s

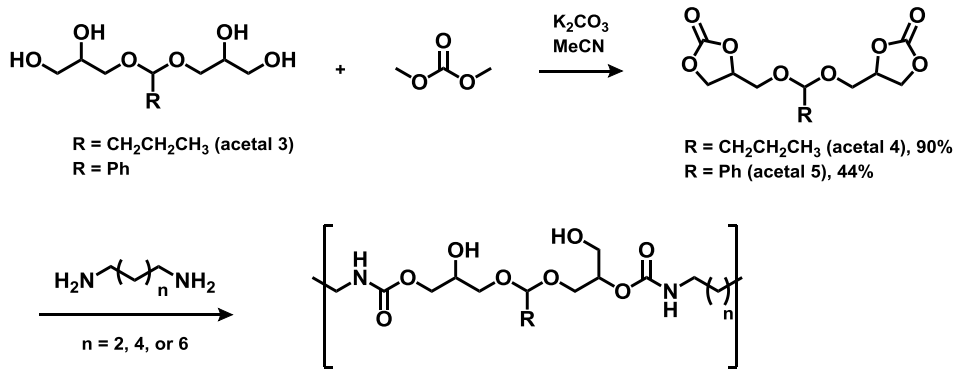

Scheme 3.6. Polymerization of poly(hydroxyurethane-acetal) by ring opening condensation of a dicarbonate acetal and a diamine.

Having demonstrated the thermal stability of **1** and its acid degradability in contact with minimal water, we proceeded to assess the polymerizations of three commercially available alkyl diamines (tetra-, hexa-, and octamethylenediamines, respectively abbreviated as TMDA, HMDA,

and OMDA) with dicarbonate acetal monomer (**4**). As can be seen from **Scheme 3.6**, monomer **4** was prepared in 90% from tetraol **3** by reacting with dimethylcarbonate in the presence of potassium carbonate as a base catalyst. Screening experiments showed poly(HU-acetal) linear polymers derived from **4** were best synthesized neat under nitrogen at 80 ^{o}C, with HMDA as the diamine and 5 mol% DABCO as the catalyst to give the highest molecular weight with a reasonable polydispersity (**Table 3.1**, bolded).

Table 3.1. Polymerization conditions for linear poly(hydroxyurethane acetal)

Amine	Solvent	Catalyst	Temp (C°)	Time (h)	M_n (kDa)*	PDI
HMDA	DMF	-	100	24	2.71	1.14
HMDA	DMF	-	RT	24	2.78	1.15
HMDA	neat	-	100	24	3.65	1.54
HMDA	neat	-	RT	24	2.77	1.15
HMDA	neat	-	RT	16	3.46	1.28
HMDA	neat	-	80	16	6.62	2.04
HMDA	THF	-	RT	18	3.03	1.19
HMDA	neat	-	85	19	3.45	1.40
HMDA	neat	Thiourea	80	16	6.84	1.41
HMDA	**neat**	**DABCO**	**80**	**16**	**8.39**	**1.60**
TMDA	neat	-	80	16	3.60	1.25
TMDA	neat	Thiourea	80	16	3.33	1.22
TMDA	neat	DABCO	80	16	4.28	1.36
OMDA	neat	-	80	16	4.12	1.37
OMDA	neat	Thiourea	80	16	-	-
OMDA	neat	DABCO	80	16	3.84	1.31

* PS standards calibration used for easier comparison to literature results

Scaled up polymerizations with > 100 mg HMDA (**Table 3.2**) gave polymers with M_n up to 50 kDa (calibrated to PS standards), possibly because a better stoichiometric control was attained with larger amounts of starting materials. A portion of these experiments utilized 1.00 ±

0.02 equivalence of monomer **4** to test the sensitivity of the polymerization to stoichiometric imbalance. The largely consistent molecular weights (**Figure 3.5**) suggested the degrees of polymerization were not severely reduced by small deviations from stoichiometric balance, although additional replications will be needed to confirm the reliability of the observations. It is also worth noting that the benzyl acetal dicarbonate monomer **5** (synthesized by Brittany Walker) appeared to polymerize with comparable efficiency as the butyl acetal monomer **4**.

Table 3.2. Scaled-up polymerization with buytl and benzyl dicarbonates

Dicarbonate	Amine	Solvent	Catalyst	Temp (C°)	Time (h)	Mn (kDa)	PDI
Butyl **4**	HMDA (1.02 eq.)	neat	DABCO	80	20	37.1	1.42
	HMDA (1.00 eq.)	neat	DABCO	80	20	48.0	1.52
	HMDA (0.98 eq.)	neat	DABCO	80	20	50.1	2.15
Benzyl **5**	HMDA (1.00 eq.)	neat	DABCO	80	20	36.1	1.43

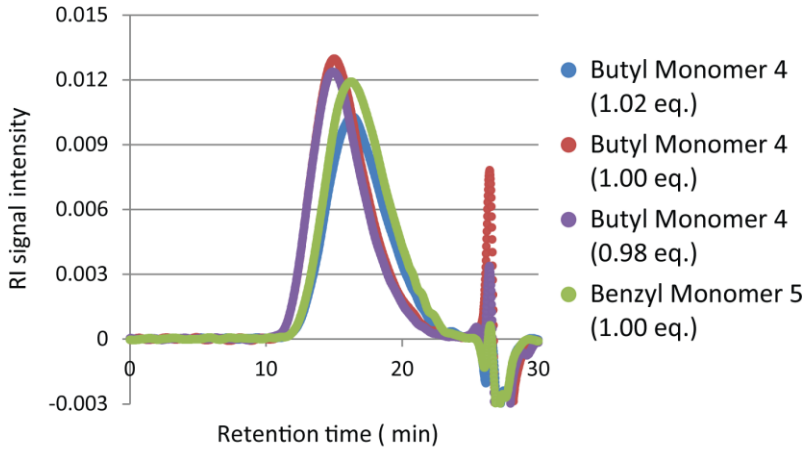

Figure 3.6. GPC traces of scaled-up linear poly(HU-acetal) polymers showing comparable retention times among polymerization using slight variations of HMDA equivalence and between those of alkyl and benzy acetal monomers.

The relative ratios of regioisomeric hydroxyurethane linkages, which typically vary between 1: 9 and 1:1 primary (1^o) to secondary (2^o) hydroxyl ratios[20], were quantified by ^{1}H and COSY NMR experiments. In the case of butyl poly (HU-acetal), a 1:3 1^o:2^o hydroxyl ratio was found as shown in **Figure 3.7**. The hydroxyl ratio in benzyl poly(HU-acetal) is under investigation.

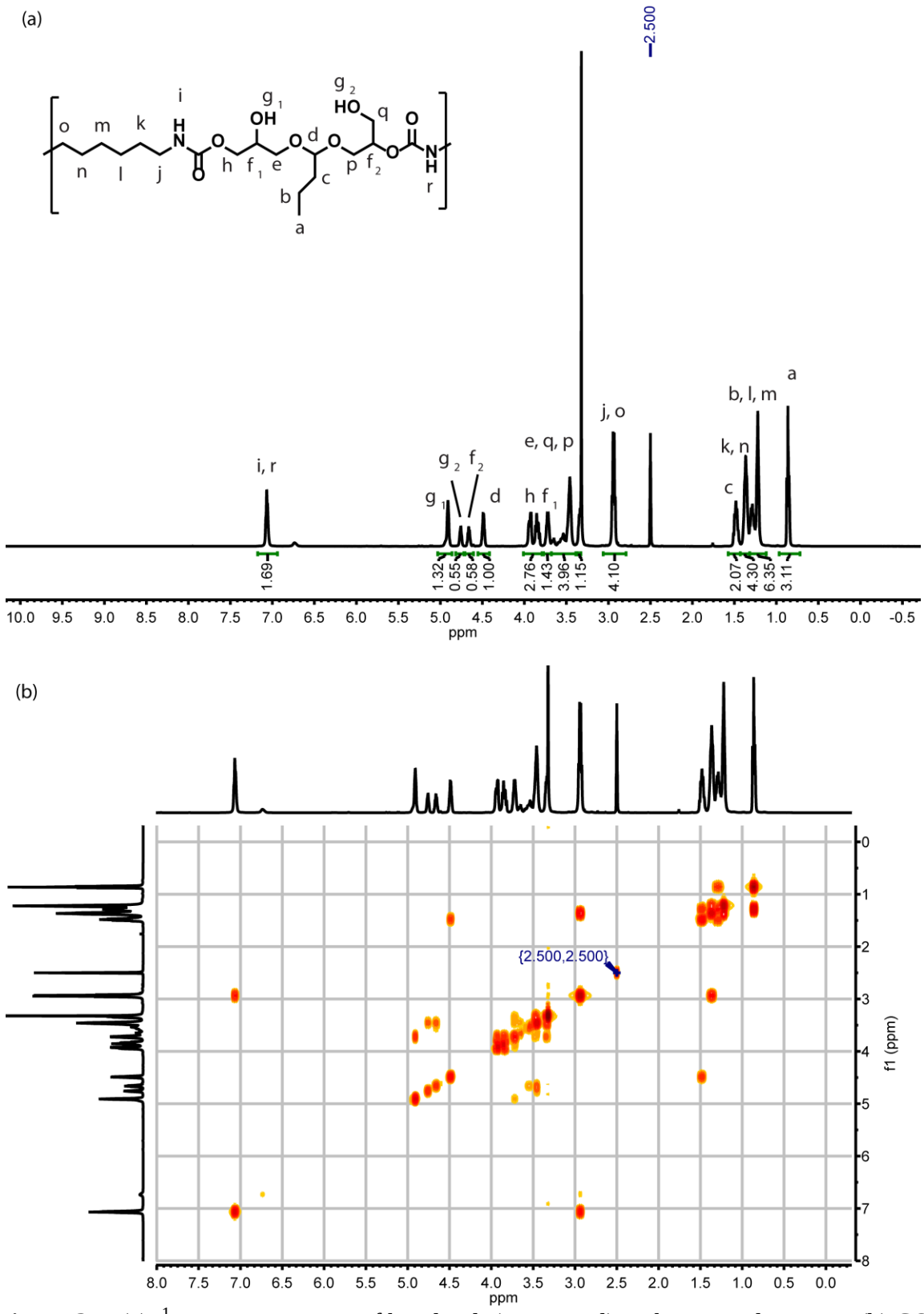

Figure 3.7. (a) ^{1}H NMR spectrum of butyl poly(HU-acetal) with assigned protons; (b) COSY spectrum of butyl poly(HU-acetal).

To confirm that the poly(HU-acetal) could depolymerize under an acidic condition, a 48 kDa poly(HU-acetal) polymer dissolved in pre-dried DMF under N_2 atmosphere to prepare a solution that was 0.1 M in acetal repeat unit and 10 mM in TsOH. At each time point, an aliquot was quenched with ~ 10 mg triethylamine, evacuated to remove residual solvent, and diluted to make ~ 30 mg/mL polymer solution for GPC injection. A control experiment with a 60 kDa poly(urethane-acetal), synthesized as shown in **Scheme 3.7**, was conducted in a similar fashion for comparison.

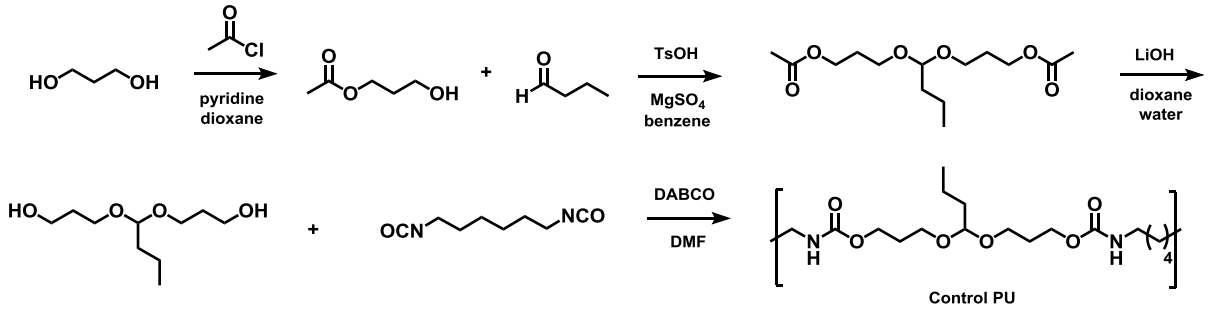

Scheme 3.7. Synthesis of control poly(urethane-acetal) without pendant hydroxyls.

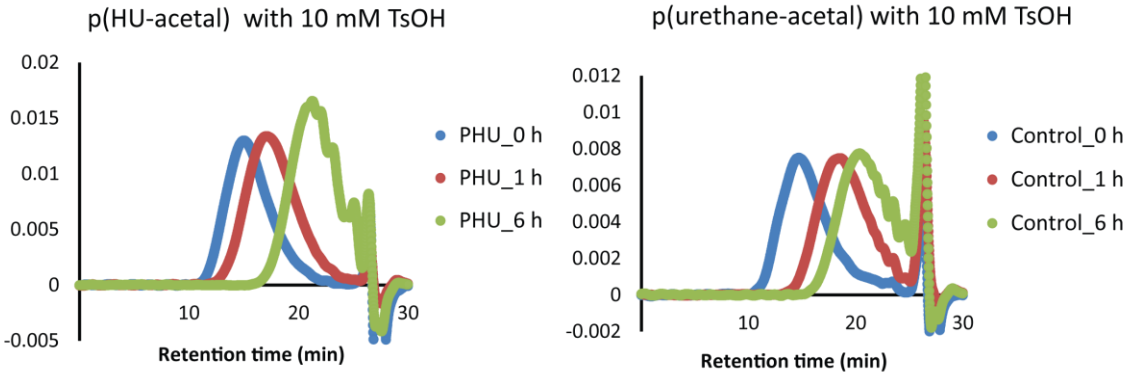

Figure 3.8. GPC traces of poly(HU-acetal) and poly(urethane-acetal) in acidic DMF solution.

The GPC traces of poly(HU-acetal) and poly(urethane-acetal) after different durations of exposure to TsOH were shown in **Figure 3.8**, which shows increasing retention times of poly(HU-acetal) with increased exposure to acid and thus indicating polymer fragmentation. However, the control polymer, which carries no pendant hydroxyls, appeared to also

depolymerize and at a slightly faster initial rate. While these preliminary results were contrary to initial prediction, some possible causes, such as incomplete drying of all species in the experiments and the design of the control polymer, need to be further investigated. An alternative structure for the control polymer is shown in **Scheme 3.8**, which better resembles the poly(HU-acetal) structure with an electron withdrawing pendant methoxy group in place of a hydroxyl.

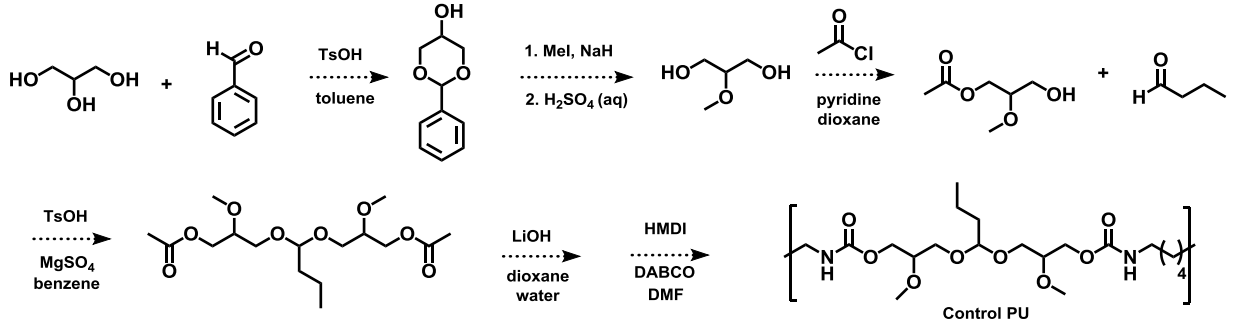

Scheme 3.8. Synthesis of alternative control poly(urethane-acetal) with pendant methoxy groups.

3.5 Crosslinked poly(hydroxyurethane-acetal) microcapsules

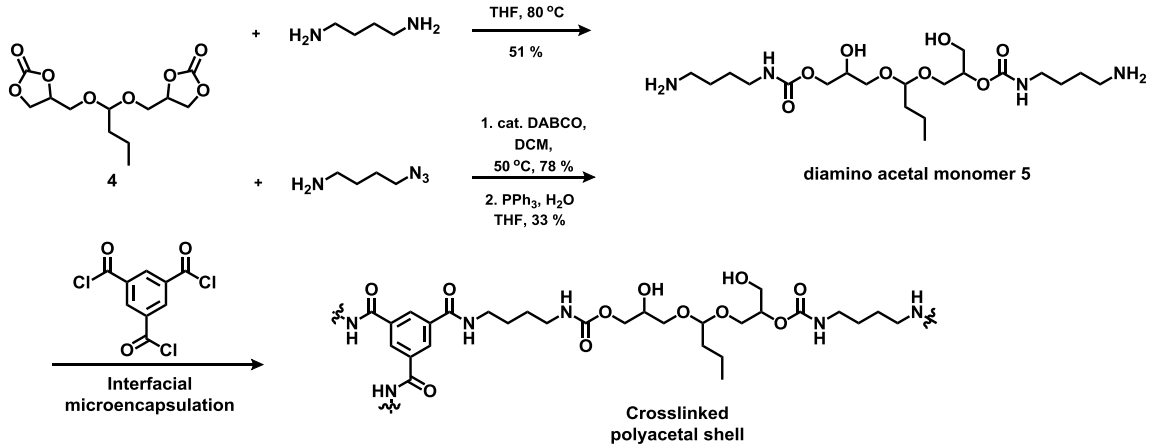

Scheme 3.9. Syntheses of diamino acetal monomer **5** and crosslinked polyacetal microcapsule.

To incorporate poly(HU-acetal) chemistry into a polymeric core-shell microcapsule, method 2 from **Scheme 3.3** was utilized to prepare polyamide microcapsules using interfacial

polymerization. The synthetic scheme is detailed in **Scheme 3.9**. Diaminobutane was selected as the smallest linker to reduce the distance between the crosslinking monomer for tighter packing and to minimize chances of premature intramolecular attack on the carbamate, which is favored for diamines with 2 or 3 methylene through the formation of 5- or 6-member cyclic urea that would lead to cleavage of the carbamate linkage. Because the water soluble, diamine-terminated HU-acetal monomer (**5)** was linear in nature, trimesoyl chloride, a crosslinker that has been demonstrated to be efficient for interfacial polymerization and microencapsulation[21,22], was selected as the hydrophobic crosslinking monomer to impart enhanced barrier properties.

Initial attempts (by Ephraim Morado) to prepare HU-acetal monomer **5** relied on mono-TFA- or mono-CBz-protected diaminobutane to ring open the carbonate groups on acetal **4**. The syntheses of TFA or CBz-terminated HU-acetal compounds either led to significant side reactions or poor conversion that rendered purification challenging. A one-step, highly scalable method to directly react acetal dicarbonate **4** with excess diaminobutane in dry THF yielded cleaner reaction mixture but the subsequent removal of residual diaminobutane by a combination of distillation and silica column chromatography remained a challenge and only afforded low amounts of the pure product. An alternative method, although requiring two extra but scalable steps from literature[23], utilized Staudinger reduction of diazide-terminated HU-acetal to prepare monomer **5** with more efficient purification.

The synthesis of oil-core poly(HU-acetal) microcapsules followed a modified literature procedure[21] : an aqueous solution of HU-acetal monomer **5** was added dropwise to a trimesoyl chloride containing oil-in-water emulsion to initiate polymerization at the droplet interface. Initial syntheses utilized toluene as the hydrophobic core solvent but the purified microcapsules showed signs of buckling, especially under high vacuum environment of SEM analysis.

Replacing toluene with Solvesso 200, a mixture of high boiling, industrial grade aromatic solvents, afforded spherical microcapsules that resisted collapse. SEM analysis of the shell cross-section of the microcapsule (**Figure 3.9**) indicated a rather smooth surface on both sides of microcapsules and shell thicknesses between 1 -3 µm.

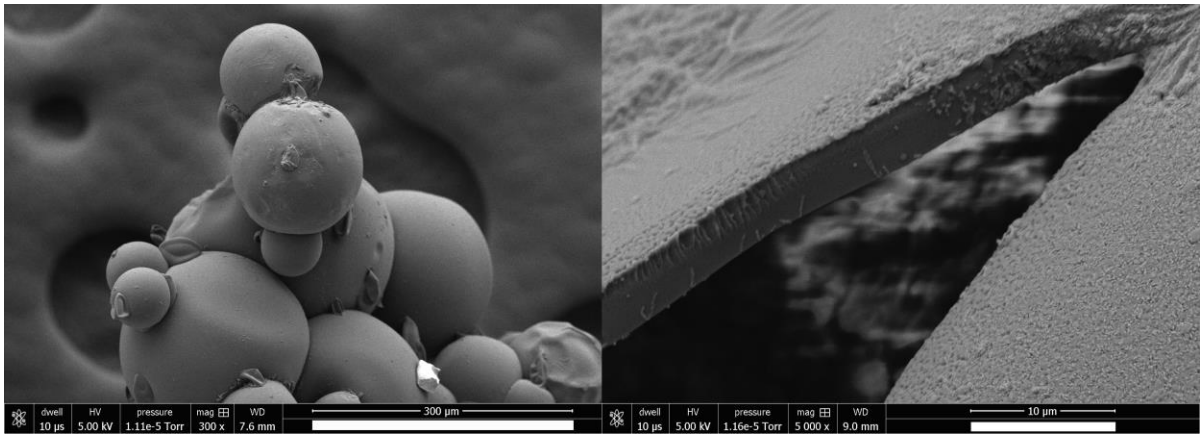

Figure 3.9. SEM images of poly(HU-acetal) microcapsules (left, scale bar: 300 µm) and shell cross-sectional view (right, scale bar: 10 µm).

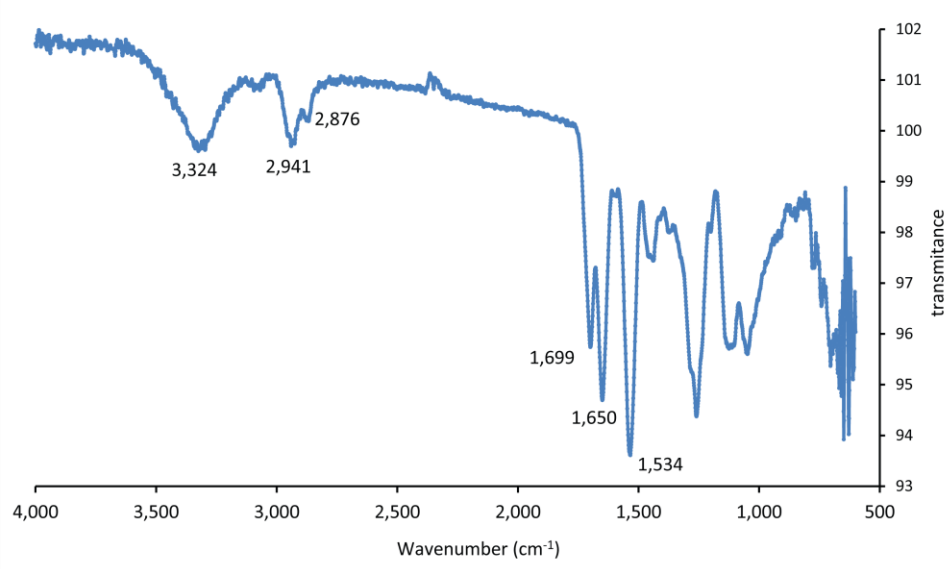

Figure 3.10. Solid state IR analysis of microcapsules shell showed presence of urethane and amide groups but no observable signal for ester.

To determine the chemical composition of the shell, and particularly to see if ester was formed during the polymerization, microcapsules were mechanically crushed, vacuum filtered, rinsed with solvents (methanol, acetonitrile, diethyl ether, and hexanes), and dried on high vacuum before the polymer fragments were analyzed on a solid state ATR FT-IR instrument. As shown in **Figure 3.10**, characteristic peaks[24] for urethane (1699 cm^{-1}), amide (amide I & II, 1650 and 1534 cm^{-1}), and hydroxyl (broad, 3324 cm^{-1}) were identified, while no visible ester signal (ca. 1800 – 1750 cm^{-1}) was detected, suggesting the hydroxyl groups critical to the proposed degradation mechanism were not consumed in any significant extent during capsules synthesis.

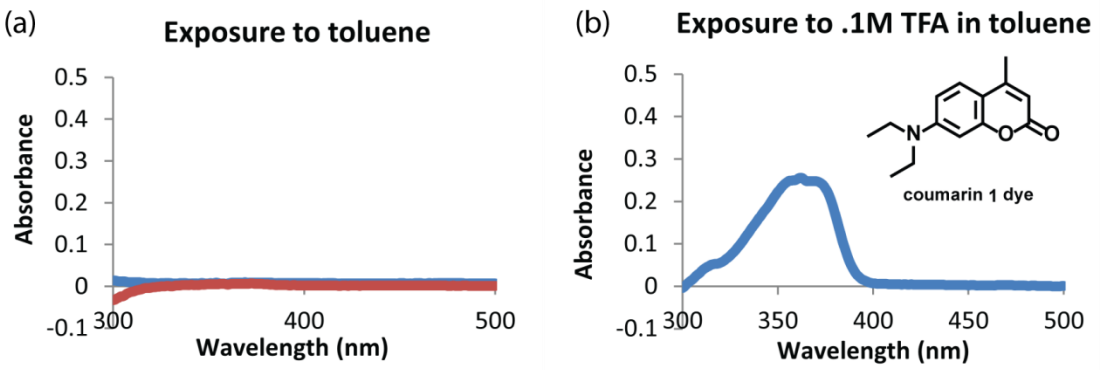

Figure 3.11. UV-vis traces of (a) exposure to toluene showing no release of dye over 2 days, and (b) exposure to 0.1 M TFA in toluene showing dye release after 1 h.

As a preliminary test for the acid degradability of the microcapsules in hydrophobic oil, dried microcapsules containing coumarin 1 dye was suspended in both toluene and a 0.1 M TFA in toluene solution. While capsules incubated in toluene remained unchanged over two days and no amount of coumarin-1 dye could be detected by UV-Vis (**Figure 3.11a**), the complete dissolution of the microcapsules in the TFA solution within 2 h suggested efficient degradation of the microcapsules under an acidic hydrophobic environment. The TFA solution post dissolution of the microcapsules was washed with 5 w/v% sodium bicarbonate solution and

subsequent UV-Vis analysis indicated presence of coumarin-1 dye, thereby confirming release of the encapsulated dye (**Figure 3.11b**).

The confirmation of acid degradability of poly(HU-acetal) microcapsules encouraged us to encapsulate 2-(4-methoxystyryl)-4,6-bis(trichloromethyl)-1,3,5-triazine, a hydrophobic photo-acid generator (PAG), in the core of the microcapsules to introduce photo-triggered degradation and release. Photo-triggered release is advantageous because of the temporal and spatial control possible with modern optical technology. Furthermore, the ubiquity of natural and artificial light sources allowed photo-initiated polymer degradation to be useful for applications such as sun light triggered release of agricultural agents.

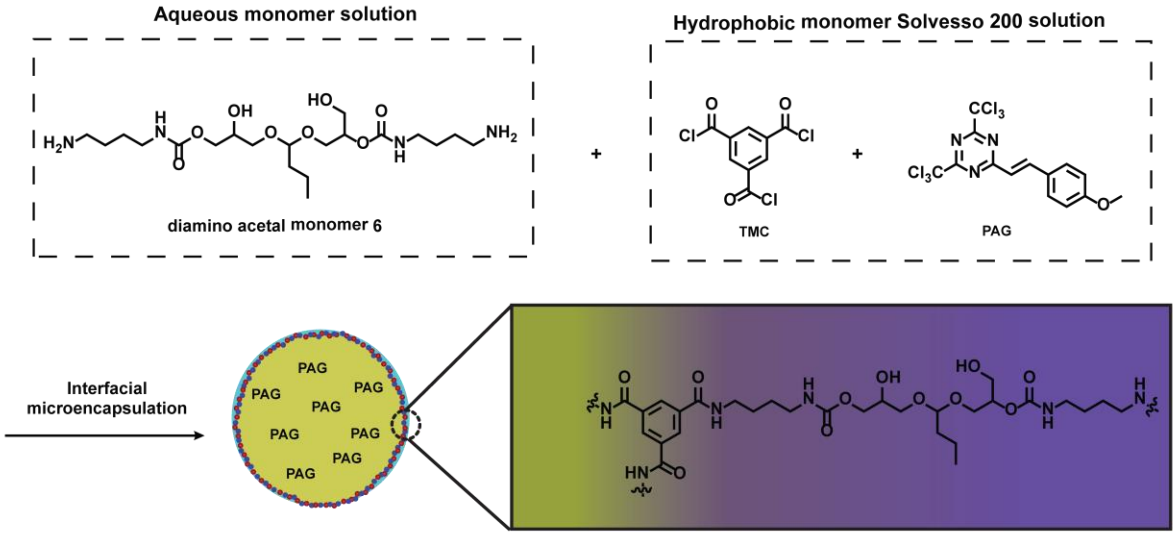

Scheme 3.10. Synthesis of PAG-loaded p(HU-acetal) microcapsules.

The encapsulation of a photoacid generator for photo-triggered degradation of an oil core polymer capsule was known in the literature[25], but there has yet to see an oil-core polyacetal microcapsule whose shell undergoes photo-triggered depolymerization at room temperature to release the core content in minutes. The synthesis of PAG-loaded microcapsules followed similar procedure (**Scheme 3.10**) as for the PAG-free microcapsules, which serve as a control.

Photolysis of the microcapsules containing 0.1 M (6 wt% in core) PAG using 365 nm LED UV demonstrated complete collapse of spherical capsular structures and the release of visible amount of Solvesso 200 liquid in 20 min. Control microcapsules containing no PAG, however, remained intact and unchanged for at least 2 h of UV irradiation. Lower amounts of encapsulated PAG, down to 0.02 M, prolonged the degradation time, offering a simple way to tune the degradation kinetics of the microcapsule for different applications.

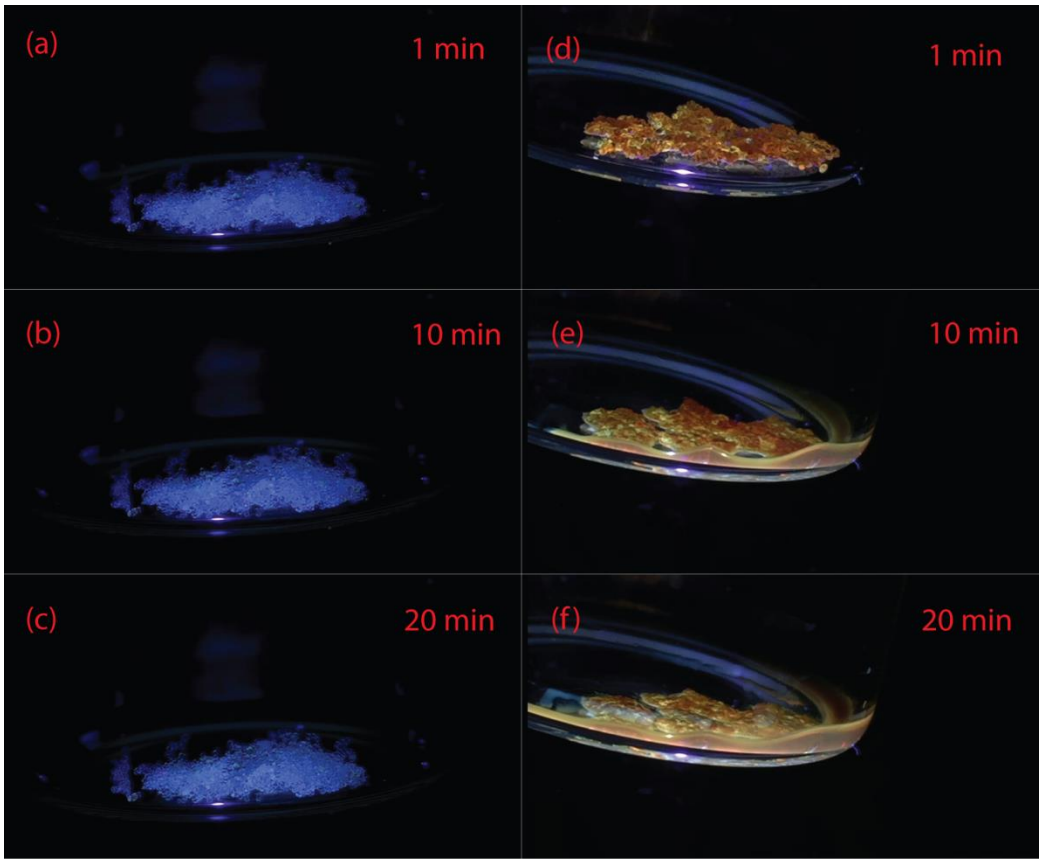

Figure 3.12. Time lapse images of UV-irradiation of (a-c) control poly(HU-acetal) microcapsules and (d-f) PAG-loaded microcapsules. PAG-loaded capsules showed UV-triggered collapse and release of core solvent with 10 min of 365 nm LED UV exposure.

3.6 Conclusion and future outlook

We proposed a new type of polyacetal capable of depolymerization through an intramolecular cyclization mechanism. The key to the polymer design is realized by a ring-opening reaction of a

cyclic carbonate that generates a pendant hydroxyl group 4 or 5 atoms away from an acetal center. As a proof of concept, a small molecule acyclic acetal structurally analogous to the repeat unit of the proposed polymer was synthesized and demonstrated to form new cyclic acetals under a low-moisture, acidic solvent environment. The linear versions of the proposed polymer were synthesized by a step-wise polymerization of a diamine and a bis(cyclic carbonate) acetal to form a poly(hydroxyurethane-acetal). Crosslinked version of the polymer was realized by interfacial microencapsulation of a diamine-terminated hydroxyurethane-acetal monomer with trimesoyl chloride. Incorporation of a hydrophobic photoacid generator in the oil core of the microcapsules allowed rapid degradation of the polymer shell by 365 nm UV and subsequent release of the encapsulated Solvesso 200 solvent within 1 h.

Future work will focus on confirming mechanism and kinetics of poly(HU-acetal) depolymerization, demonstrating tunability of degradation kinetics using different substituents, and investigate polymer physical properties to explore applications.

3.7 Experimental section

General Methods

All solvents and reagents were used as received unless otherwise noted. Anhydrous solvents were obtained from a MBraun SPS-800 Solvent Purification System. Reaction temperatures reported were the temperatures of the heating or cooling medium. Column chromatography was performed using flash silica gel (40-63 μm, 230-400 mesh). Unless otherwise noted, ^{1}H NMR and ^{13}C NMR spectra were obtained on a 500 MHz Varian instrument (U500 or VXR500) at the VOICE NMR laboratory at the University of Illinois at Urbana-Champaign. Chemical shifts are reported in parts per million (ppm) and coupling constants in Hertz (Hz). NMR spectra obtained in $CDCl_3$ were referenced to 7.26 ppm for ^{1}H and 77.16 ppm for ^{13}C; methanol-d_4 was

referenced to 3.31 ppm for ^{1}H and 49.00 ppm for ^{13}C; DMSO-d_6 was referenced to 2.50 ppm for ^{1}H and 39.52 ppm for ^{13}C. ESI mass spectra were obtained at the Mass Spectrometry Center at the University of Illinois at Urbana-Champaign. UV-visible spectroscopic measurements were performed on a Shimadzu UV-2501PC instrument using a 1.5 mL quartz cuvette with a path length of 1 cm. FT-IR was obtained on a Nicolet Nexus 670 ATR instrument. Scanning electron microscopy was performed on an FEI^{TM} Quanta FEG 450 environmental scanning electron microscope at the Imaging Technology Group of the Beckman Institute at the University of Illinois at Urbana-Champaign. A Thorlabs M365L2 365 nm LED UV (190 mW min., 700 mA) was used for the UV-triggered microcapsules degradation experiments. Polymer molecular weight determination was carried out at 50 ^{o}C on a Waters GPC instrument composed of a Waters 1515 isocratic pump, a Waters 2414 refractive index detector, and a miniDAWNTREOS 3-angle laser light scattering detector. The GPC eluent was 0.45 μm-filtered 0.1 M LiBr in HPLC grade DMF.

Synthetic Procedure

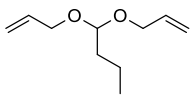

Butyraldehyde diallyl acetal **1**. The synthesis of acetal **1** of was based on literature[26] reported procedure. A solution of 80 mL (0.89 mol) butyraldehyde and 95 mL (1.4 mol) allyl alcohol in 320 mL hexanes was added 71 g $MgSO_4$ and 2.64 g (0.0139 mol) *p*-toluenesulfonic acid monohydrate. The suspension was stirred at room temperature for 18 h and quenched by adding an aqueous solution of 2 g K_2CO_3 in 320 mL DI water. The biphasic solution was separated and the organic layer was furthered washed with 80 mL of 1 w/v% aqueous solution of $NaHCO_3$, 100

mL of brine, and dried over Na_2SO_4. Concentration invacuo yielded 92 g of a slightly yellowish clear oil that was fractionally distillated at 50 torr and 104-106 ℃ to afford 76.4 g (64%) colorless oil. ^{1}H NMR ($CDCl_3$): δ 5.94 (ddt, *J* = 17, 10.5, 5.5, 2H), 5.31 (ddt, *J* = 16.5, 1.5, 1.5, 2H), 5.18 (ddt, *J* =10, 1.5, 1.5, 2H), 4.63 (t, *J* = 6, 1H), 4.11 (ddt, *J* = 12.5, 5, 1.5, 2H), 4.03 (ddt, *J* = 12.5, 5, 1.5, 2H), 1.690-1.616 (m, 2H), 1.42 (sextet, *J* = 7.5, 2H), 0.95 (t, *J* = 7.5, 3H). ^{13}C NMR ($CDCl_3$): δ 134.9, 116.8, 102.1, 66.2, 35.6, 18.2, 14.1.

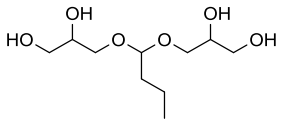

Butyraldehyde bis(2,3-dihydroxypropyl) acetal **3**. Standard Upjohn dihydroxylation condition was employed for the synthesis of tetrol acetal **3**. A solution of 8.4 g (49 mmol) diallyl acetal **1** in 120 mL acetone was added 35 mL aqueous *N*-methylmorpholine oxide solution (52 wt% NMO) and 70 mg (0.19 mmol) potassium osmate dihydrate. The solution was stirred for 18 h at room temperature. To quench the reaction, 5 g Na_2SO_3 was added and the suspension stirred for 2.5 h. The suspension was vacuum filtered and solid residue was rinsed with small portions of methanol. The filtrate was concentrated in vacuo to give 32 g of brown oil that was washed with 100 mL hexanes three times. Attempts to extract with 100 mL 50% v/v isopropanol in chloroform or with 50 mL ethyl acetate did not lead to phase separation. The single phase solution was concentrated in vacuo and lyophilized to remove excess water solvent. The residue was roughly purified by silica column chromatography with 0.2 v/v% trimethylamine in 10 vol% methanol in dichloromethane to afford 8.5 g of a brown oil that was confirmed by NMR to be mostly the desired product. The viscous product containing oil was used in subsequent reaction without further purification. ^{1}H NMR (CD_3OD): δ 4.58 (m, 1H), 3.78-3.71 (m, 2H), 3.69-3.43 (m,

8H), 1.690-1.616 (m, 2H), 1.41 (sextet, J = 7.5, 2H), 0.94 (t, J = 7.5, 3H). ESI-HRMS: calculated 261.1314, found 261.1301, $C_{10}H_{22}O_6Na$ $[M+Na]^+$.

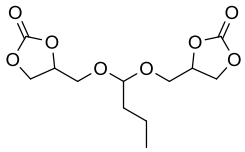

Butyraldehyde dicarbonate acetal **4**. In a three-neck 100 mL round bottom flask, a solution of 4.0 g (17 mmol) tetraol acetal **3** in 15 mL acetonitrile was added 13 mL (154 mmol) dimethyl carbonate and 2 g K_2CO_3 granules. The stirring suspension was refluxed under N_2 for 2.5 h. An additional 12 mL (142 mmol) dimethyl carbonate was added and the oil heating bath was turned down to 50 ^oC. The suspension was cooled after 11.5 h, diluted with 50 mL dichloromethane, vacuum filtered to remove the solids, and the clear filtrate was concentrated in vacuo to yield 6 g of viscous brown oil. Further purification by elution through a silica plug (4 cm in diameter, 6 cm in height) with an eluent of 0.1 v/v% triethylamine in 1 vol.% methanol in dichloromethane afforded, upon solvent removal, 4.4 g (90%) of a viscous yellow oil. Note: NMR analysis showed overlapping peaks that are consistent with the expected structures, suggesting presence of isomeric products. ^1H NMR ($CDCl_3$): δ 4.92-4.80 (m, 2H), 4.70-4.61 (m, 1H), 4.56-4.47 (m, 2H), 4.47-4.29 (m, 2H), 3.91-3.77 (m, 2H), 3.73-3.56 (m, 2H), 1.65-1.54 (m, 2H), 1.43 – 1.29 (m, 2H) 0.96-0.87 (m, 3H). ^{13}C NMR ($CDCl_3$): δ 155.11, 155.07, 130.3, 103.1, 103.0, 75.20, 75.15, 75.11, 75.0, 66.14, 66.08, 66.03, 65.3, 64.1, 63.8, 63.4, 34.8, 34.7, 34.6, 18.0, 17.9,17.86, 13.92, 13.90. ESI-HRMS: calculated 313.0899, found 313.0905, $C_{12}H_{18}O_8Na$ $[M+Na]^+$.

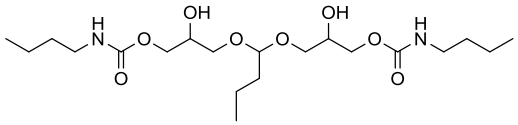

Hydroxyurethane-acetal **1**. To a 15 mL round bottom flask, 0.477 g (2.00 mmol) tetraol **3** and 8 mg (0.07 mmol) DABCO catalyst were added. The flask was evacuated and filled with nitrogen. The suspension was added 0.45 mL (4.0 mmol) n-butylisocyanate via a syringe and stirred for 1 h, which remained slightly turbid. Addition of 1 mL anhydrous dichloromethane formed a clear solution that was allowed to stir overnight under nitrogen. The solution was concentrated in vacuo and purified by silica column chromatography using gradient elution with 50 to 100% ethyl acetate in hexanes to isolate the third major TLC spot as 83 mg (9%) of a clear viscous oil. Note: the broadened and complex NMR peaks with the expected shifts and consistent integrals suggested an isomeric mixture was obtained after purification. ^{1}H NMR ($CDCl_3$): δ 5.23 (s br, 2H), 4.58-4.51 (m, 1H), 4.26-4.06 (m, 4H), 4.02-3.90 (m br, 2H), 3.66-3.48 (m, 4H), 1.46 (pent, *J* = 7.5, 4H), 1.32 (sextet, *J* = 7.5, 6H), 0.90 (t, *J* = 7.5, 9H). ^{13}C NMR ($CDCl_3$): δ 157.2-157.0, 103.4-103.1, 69.7-39.3, 66.3-65.8, 60.5, 40.9, 35.1, 32.0, 20.0, 18.0, 14.3. ESI-HRMS: calculated 459.2682, found 459.2672, $C_{20}H_{40}N_2O_8Na$ $[M+Na]^+$

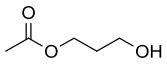

3-hydroxypropyl acetate. The synthesis of 3-hydroxypropyl acetate followed literature procedure[27] to afford 3.8 g of a yellow oil in 16% yield. ^{1}H NMR ($CDCl_3$): δ 4.19 (t, *J* = 6, 2H), 3.66 (t, *J* = 6, 2H), 2.03 (s, 3H), 1.84 (quintet, *J* = 6, 2H). ^{13}C NMR ($CDCl_3$): δ 171.7, 61.5, 59.1, 31.7, 21.0. ESI-HRMS: calculated 141.0528, found 141.0525, $C_5H_{10}O_3Na$ $[M+Na]^+$

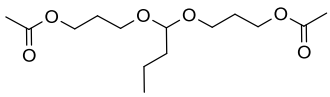

Acetyl-protected Butyraldehyde bis(3-hydroxypropyl) acetal. To a 15 mL round bottom flask, 0.48 g (4.1 mmol) and 0.54 mL (6.0 mmol) butyraldehyde were added and dissolved in 2 mL benzene under nitrogen. The solution was added 0.55 g $MgSO_4$ and 13 mg (0.0139 mmol) *p*-toluenesulfonic acid monohydrate and stirred at room temperature for 9 h. The suspension was added 1 mL trimethylamine, diluted with 5 mL dichloromethane, and vacuum filtered. The filtrate was washed with 10 mL of 5 w/v% aqueous $NaHCO_3$, 10 mL of brine, dried over Na_2SO_4 and concentrated invacuo to give 0.57 g of a clear oil that was further purified by silica column chromatography using gradient elution of 15 to 25 vol% ethyl acetate in hexanes to afford 0.44 g (75%) of a clear, slightly yellow oil. ^{1}H NMR ($CDCl_3$): δ 4.47 (t, *J* = 6, 1H), 4.16 (t, *J* = 6.5, 4H), 3.63 (dt, *J* = 6, 10, 2H), 3.47 (dt, *J* = 6, 10, 2H), 2.04 (s, 6H), 1.88 (quintet, *J* = 6.5, 4H), 1.60-1.54 (m, 2H), 1.35 (sextet, *J* = 7, 2H), 0.91 (t, *J* = 7.5, 3H). ^{13}C NMR ($CDCl_3$): δ 171.3, 103.3, 61.9, 61.87, 35.5, 29.3, 21.2, 18.3, 14.2. ESI-LRMS: calculated 313.2, found 313.3, $C_{14}H_{26}O_6Na$ $[M+Na]^+$

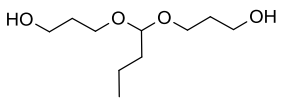

Butyraldehyde bis(3-hydroxypropyl) acetal. To a 10 mL round bottom flask, 0.1 g (0.35 mmol) of (9-56) and 0.06 g (3 mmol) LiOH were added and suspended in 1.2 mL of a 50:50 volume ratio solution of 1,4-dioxane and DI water. The suspension was stirred for 3 h at room temperature. Dropwise addition of ca. 1.6 mL 1 M aqueous HCl solution lowered the pH to ca. 8 as indicated by a pH paper. The solution was concentrated to ~ 1 mL of cloudy suspension that was extracted with 3 mL ethyl acetate three times. The combined organic layer was dried over

Na_2SO_4 and concentrated invacuo to afford 68 mg (96%) of a clear oil. ^{1}H NMR ($CDCl_3$): δ 4.50 (t, *J* = 6, 1H), 3.80-3.71 (m, 6H), 3.64-3.56 (m, 2H), 2.82 (s br, 2H), 1.82 (p, *J* = 5.5, 4H), 1.63-1.55 (m, 2H), 1.36 (sextet, *J* = 7.5, 2H), 0.92 (t, *J* = 7.5, 3H). ^{13}C NMR ($CDCl_3$): δ 103.3, 63.8, 61.1, 35.4, 32.3, 18.1, 14.1. ESI-HRMS: calculated 229.1416, found 229.1410, $C_{10}H_{22}O_4Na$ $[M+Na]^+$

General procedure for HMDA-dicarbonate polymerizations

Hexamethylenediamine from commercial bottle was freshly recrystallized from cyclohexane (ca. 13 g in 100 mL), stored and handled under nitrogen in a glovebag. For each polymerization, the exact amount of catalyst and dicarbonate acetal monomer used was determined by the amount of diamine placed in a tared 20 mL glass vial under nitrogen in glove bag. Liquid catalysts are added by direct injection with a syringe. Solid catalyst was injected as a stock solution of known concentration in anhydrous THF. Stoichiometric amount of the dicarbonate acetal monomers were weighed out in a separate 20 mL vial, flushed with nitrogen and placed in the glovebag for dissolution in anhydrous THF. The dissolved dicarbonate solution and catalyst liquid/solution were injected to the vial containing the diamine. The dicarbonate-containing vail was rinsed with same portion of anhydrous THF five times to ensure complete transfer of monomer. The dissolved monomers and catalyst solution was transferred via syringe to a 20 mL vial that is outside the glovebag under positive nitrogen pressure and contains a stir bar. Concentration of the reaction solution under vacuum removed the THF solvent until the viscosity of mixture stopped the stirring. The vial under nitrogen was heated in an oil bath for the desired amount of time. For purification, the residue was dissolved in anhydrous THF under nitrogen and precipitated at least 3 times in anhydrous diethyl ether (volume ratio 1:9 THF:diethyle ether). The collected solid was dried by high vacuum and analyzed by NMR and GPC.

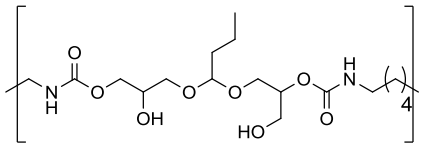

To a 20 mL vial with a stir bar under nitrogen, 0.201 g HMDA was added a solution of 0.501 g acetal **4** in 0.5 mL anhydrous THF and 0.49 mL of 6 mg/mL DABCO for a mole ratio of 1 diamine :1 dicarbonate:0.05 catalyst. Five portions of 0.5 mL anhydrous THF rinsed and transferred all butyl acetal. The solution was concentrated and heated for 20 h at 80 ^{o}C. The residue was dissolved in 5 mL anhydrous THF and precipitated in 45 mL diethyl ether three times. Drying on high vacuum afforded 0.7 g of a sticky, yellowish white solid. d_n/d_c = 0.063, M_n = 48.0 (PS standard) and 10.1 kDa (LS); PDI = 1.52 (PS standard) and 1.66 (LS).

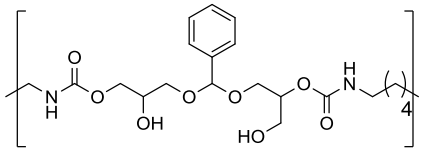

To a 20 mL vial with a stir bar under nitrogen, 0.090 g HMDA was added a solution of 0.252 g acetal **5** in 0.5 mL anhydrous THF and 0.22 mL of 6 mg/mL DABCO for a mole ratio of 1 diamine :1 dicarbonate:0.05 catalyst. Five portions of 0.5 mL anhydrous THF rinsed and transferred all butyl acetal. The solution was concentrated and heated for 20 h at 80 ^{o}C. The residue was dissolved in 5 mL anhydrous THF and precipitated in 45 mL diethyl ether three times. Drying on high vacuum afforded 0.7 g of a sticky, yellowish white solid. d_n/d_c = 0.087, M_n = 36.1 (PS standard) and 9.2 kDa (LS); PDI = 1.43 (PS standard) and 1.39 (LS).

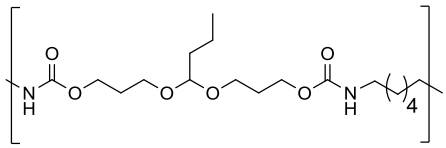

To a 10 mL round bottom flask under nitrogen, 0.235 g (1.14 mmol) diol acetal was added and dissolved in 3 mL anhydrous *N,N*-dimethylformamide. The stirring solution was added 0.183 mL hexamethylene diisocyanate via microsyringe and ca. 15 mg dibutyltin dilaurate catalyst. The solution was heated at 70 ^{o}C for 32 h, cooled to room temperature, and precipitated in 45 mL diethyl ether three times. The solid was dried on high vacuum to afford 0.26 g of a white, slightly waxy powder. d_n/d_c = 0.0507, M_n = 59.8 (PS standard) and 13.8 kDa (LS); PDI = 1.45 (PS standard) and 1.72 (LS).

UV-triggered microcapsules degradation

The UV degradation experiment of the PAG-loaded poly(HU-acetal) microcapsules was conducted in a capped 20 mL glass vial. The 365 nm UV LED lamp was position directly beneath the vial at a distance of ca. 3 cm. The illumination was set to the maximum power throughout the experiment.

3.8 References

(1) Cordes, E. H.; Bull, H. G. *Chem. Rev.* **1974**, *74*, 581.

(2) Binauld, S.; Stenzel, M. H. *Chem. Commun.* **2013**, *49*, 2082.

(3) Liu, B.; Thayumanavan, S. *J. Am. Chem. Soc.* **2017**, *139*, 2306.

(4) Kreevoy, M. M.; Morgan, C. R.; Taft, R. W. *J. Am. Chem. Soc.* **1960**, *82*, 3064.

(5) Paramonov, S. E.; Bachelder, E. M.; Beaudette, T. T.; Standley, S. M.; Lee, C. C.; Dashe, J.; Fréchet, J. M. J. *Bioconjugate Chem.* **2008**, *19*, 911.

(6) Deslongchamps, P.; Dory, Y. L.; Li, S. *Tetrahedron* **2000**, *56*, 3533.

(7) Li, S.; Dory, Y. L.; Deslongchamps, P. *Isr. J. Chem.* **2000**, *40*, 209.

(8) DeWit, M. A.; Gillies, E. R. *J. Am. Chem. Soc.* **2009**, *131*, 18327.

(9) Dewit, M. A.; Beaton, A.; Gillies, E. R. *J. Polym. Sci., Part A: Polym. Chem.* **2010**, *48*, 3977.

(10) Chen, E. K. Y.; McBride, R. A.; Gillies, E. R. *Macromolecules* **2012**, *45*, 7364.

(11) de Gracia Lux, C.; Almutairi, A. *ACS Macro Letters* **2013**, *2*, 432.

(12) de Gracia Lux, C.; Olejniczak, J.; Fomina, N.; Viger, M. L.; Almutairi, A. *J. Polym. Sci., Part A: Polym. Chem.* **2013**, *51*, 3783.

(13) Geschwind, J.; Frey, H. *Macromolecules* **2013**, *46*, 3280.

(14) Zhang, L.-J.; Deng, X.-X.; Du, F.-S.; Li, Z.-C. *Macromolecules* **2013**, *46*, 9554.

(15) Mejia, J. S.; Gillies, E. R. *Polymer Chemistry* **2013**, *4*, 1969.

(16) Olejniczak, J.; Chan, M.; Almutairi, A. *Macromolecules* **2015**, *48*, 3166.

(17) Lv, A.; Cui, Y.; Du, F.-S.; Li, Z.-C. *Macromolecules* **2016**, *49*, 8449.

(18) Tsai, F.-T.; Wang, Y.; Darensbourg, D. J. *J. Am. Chem. Soc.* **2016**, *138*, 4626.

(19) Darensbourg, D. J.; Wei, S.-H. *Macromolecules* **2012**, *45*, 5916.

(20) Maisonneuve, L.; Lamarzelle, O.; Rix, E.; Grau, E.; Cramail, H. *Chem. Rev.* **2015**, *115*, 12407.

(21) Broaders, K. E.; Pastine, S. J.; Grandhe, S.; Frechet, J. M. J. *Chem. Commun.* **2011**, *47*, 665.

(22) Mathiowitz, E.; Cohen, M. D. *J. Membr. Sci.* **1989**, *40*, 27.

(23) Jung, M. E.; Ouk, S.; Yoo, D.; Sawyers, C. L.; Chen, C.; Tran, C.; Wongvipat, J. *J. Med. Chem.* **2010**, *53*, 2779.

(24) Lin-Vien, D.; Colthup, N. B.; Fateley, W. G.; Grasselli, J. G. In *The Handbook of Infrared and Raman Characteristic Frequencies of Organic Molecules*; Academic Press: San Diego, 1991, p 117.

(25) Siebert, J. M.; Baier, G.; Landfester, K. *J. Polym. Sci., Part A: Polym. Chem.* **2012**, *50*, 80.

(26) Nakamura, Y.; Daiichi Sankyo Company, Limited: US Patent, 2014.

(27) Dittmer, D. C.; Hertler, W. R.; Winicov, H. *J. Am. Chem. Soc.* **1957**, *79*, 4431.